Palaeobiodiversity and Palaeoenvironments
https://doi.org/10.1007/s12549-023-00585-z

SENCKENBERG

ORIGINAL PAPER

Lithofacies variability and facies analysis of a Givetian reef in the southwestern Lahn Syncline (Rhenish Massif, Germany)

Peter Königshof[1] · **Steffen Loos**[2] · **Julia Rutkowski**[2]

Received: 16 March 2023 / Revised: 11 May 2023 / Accepted: 14 June 2023

Abstract

A 200 m thick drill core penetrating the Givetian Hahnstätten Reef in the southwestern Lahn Syncline (Rhenish Massif) was investigated. A range of different depositional environments is described based on lithofacies and microfacies analysis. All in all, nine lithofacies types (FTs) are distinguished, which can include subfacies types. The majority of lithofacies of these ultrapure carbonates is represented by lime mudstone and fenestral microbialites, all pointing to shallow subtidal, intertidal to even supratidal low-energy palaeoenvironments. In contrast, more high-energy parts of the reef were dominated by bioclastic rubble deposits (e.g. rudstone). Autochthonous, reef-building carbonates are represented by bafflestone and framestone. Diversity of reef building organisms (stromatoporoids and corals) is low and is dominated by *Stachyodes*, *Actinostroma*, *Stromatopora*, and *Thamnopora* and alveolitids, respectively. Other bioclasts are brachiopods, gastropods, ostracods, foraminifera, echinoderms, trilobites, and conodonts in descending order. Development of the Hahnstätten Reef is interpreted as having been controlled mainly by synsedimentary tectonics and volcanism with contributions from eustasy. The occurrence of *Stringocephalus burtini* in the entire section and conodont findings, which provide more precise biostratigraphic data confirm an early to middle Givetian age (*Polygnathus rhenanus/varcus* Zone to *Polygnathus ansatus* Zone) of the succession. The average quality of the ultrapure carbonates lies at 97.68% CaO (excl. loss of ignition), with 70% of the core ranging between 98% and 99% CaO. This extremely high purity makes it difficult to identify correlations between lithofacies and geochemical data.

Keywords Middle Devonian · Rhenish Massif · Reef limestone · Facies · Biostratigraphy

Introduction

Middle Palaeozoic reefs appear to have peaked in abundance during the Wenlock and the Givetian-Frasnian at the highest levels of the Phanerozoic (e.g. Flügel and Kiessling 2002; Copper 2002a; Copper and Scotese 2003). Major controls of tropical carbonate environments were triggered by the intense global change during the Late Devonian and Mississippian as determined by palaeoclimate, volcanism, eustatic sea-level, and regional tectonics. Reefs globally flourished during the Middle Devonian, expanding in the late Eifelian and reaching their maximum extension during the early to middle Givetian, but finally metazoan reefs completely disappeared at the end of the Frasnian in the cause of the global Kellwasser Crisis (e.g. Hallam and Wignall 1997; Copper 2002b). In the Rhenish Massif as well as further in the west along the Ardennes Shelf, most reefs disappeared before the end Frasnian (e.g. Eder and Franke 1982; Mottequin et al. 2015; Aboussalam and Becker 2016; Becker et al. 2016a; Hartkopf-Fröder and Weber 2016; Mottequin and Poty 2016; Stichling et al. 2022). During the Middle Devonian the palaeogeographic position favoured the development of widely distributed coral/stromatoporoid reefs in the Rhenish Massif and elsewhere along the southern shelf of Laurussia. Over this favourable period several reefs in the Rhenish Massif

This article is a contribution to the special issue "The Rhenish Massif: More than 150 years of research in a Variscan mountain chain, part II".

✉ Peter Königshof
peter.koenigshof@senckenberg.de

Steffen Loos
steffen.loos@schaeferkalk.de

Julia Rutkowski
julia.rutkowski@schaeferkalk.de

[1] Senckenberg Research Institute and Natural History Museum Frankfurt, Senckenberganlage 25, 60325 Frankfurt am Main, Germany

[2] SCHAEFER KALK GmbH & Co. KG, Division for Technical & Enviromental Services, Department for Geology & Property Management, Aarstraße, 65623, Hahnstätten, Germany

Published online: 19 September 2023

attained thicknesses of almost 1000 m (e.g. Hagen-Balve Reef Complex, Attendorn Reef, Brilon Reef, Löw et al. 2022; Stichling et al. 2022), while others reached only a few hundred metres. East of the river Rhine (Lahn-Dill area) most reefs are associated with volcanic buildups, which triggered reef growth at that time (e.g. Krebs 1971; Oetken 1997; Königshof et al. 2010, 2023; Königshof and Flick in press, this issue), whereas west of the river Rhine such as in the Eifel area, platform carbonates with bioherms and mud-mounds prevail (Faber 1980; Pohler et al. 1999; Königshof et al. 2016, Fig. 1).

In the Lahn Syncline initial reef development is associated with a longer break in volcanic activity and started within the *Polygnathus ansatus* Zone at different places mainly on top of drowned volcanic buildups (Buggisch and Flügel 1992) or established even earlier in the *Polygnathus timorensis* Zone (Braun et al. 1994). In the frame of ongoing discussions on events in Earth's History, reef development and causes of extinction of metazoan reefs became again a recent research focus and some classical sections within the Rhenish Massif were revisited and studied again (e.g. Löw et al. 2022; Stichling et al. 2022; Königshof and Flick in press, this issue). This study provides a detailed lithological and facies description of a 200 m drill core through a Givetian reef limestone in the southeastern Rhenish Massif (Fig. 2), which was sank for exploration purposes. Core material was provided by SCHAEFER KALK GmbH & Co, Hahnstätten.

Methods and material

The study consisted of detailed logging at cm scale of a drill core through a Givetian reef in the southeastern Rhenish Massif (Mudershausen Formation, Lahn Syncline). Drill core HST 79 (map sheet 1:25.000, no 5614, Limburg an der Lahn, r 3433125, h 5576245; 184,14m NN) was sunk by SCHAEFER KALK GmbH & Co and reached a depth of 200,20 m. The core penetrating the Hahnstätten Reef was chosen to document reef development based on lithofacies and microfacies analysis. Drill cores were cut and polished and samples were taken for thin sections and biostratigraphy (conodont samples). In order to get a thorough overview of the facies,

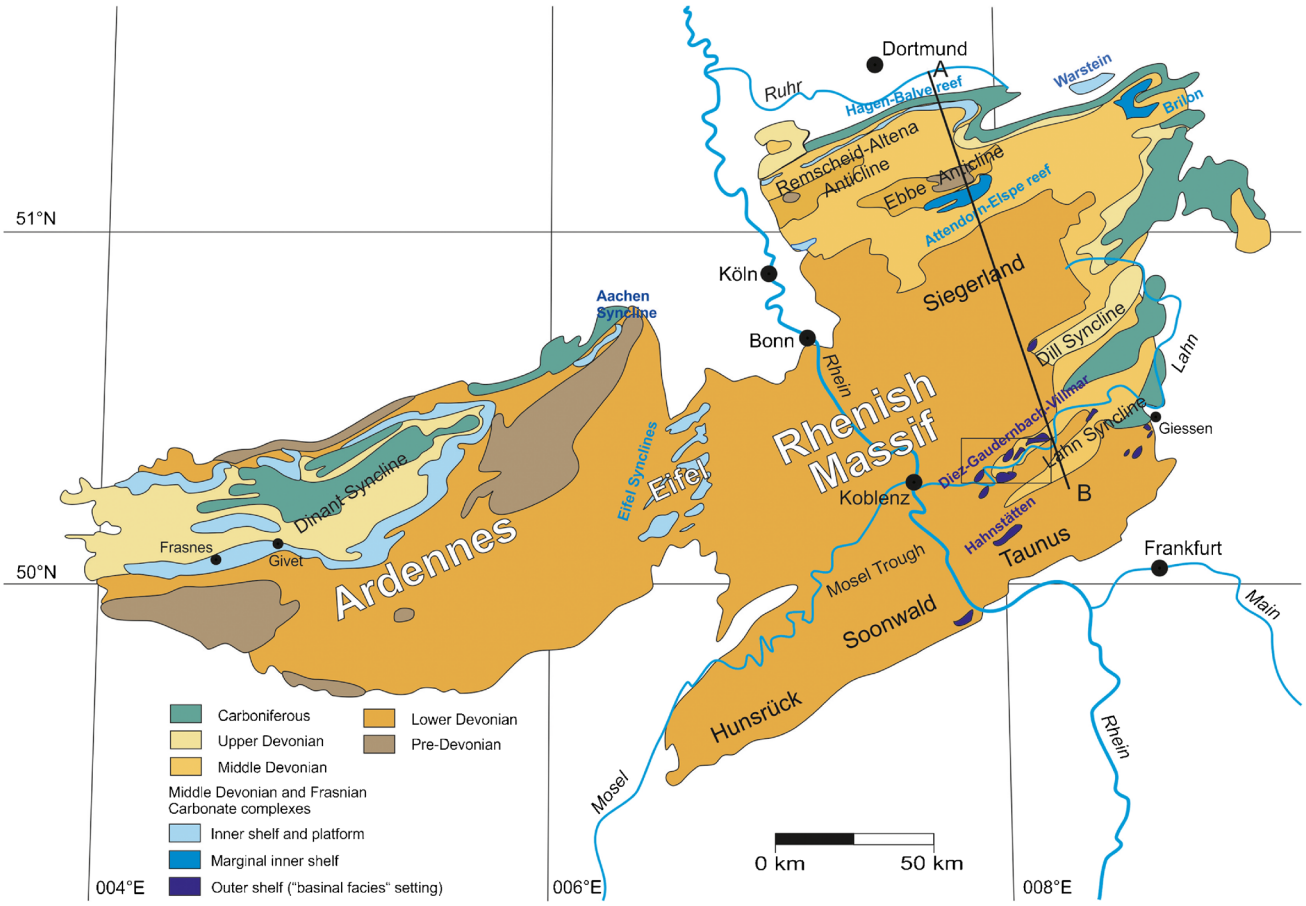

Fig. 1 Simplified geological map of Palaeozoic rocks of the Ardennes and the Rhenish Massif with the distribution of reefs in different shelf settings. Reef structures at the inner shelf and at the marginal inner shelf have been mainly established on siliciclastic sediments (not exclusively), whereas reef development in the southern Rhenish Massif is linked with volcanic sediments and volcanoes as a result of crustal extension. Rectangle shows position of figure 2. Modified after Wehrmann et al. (2005) and Königshof et al. (2023)

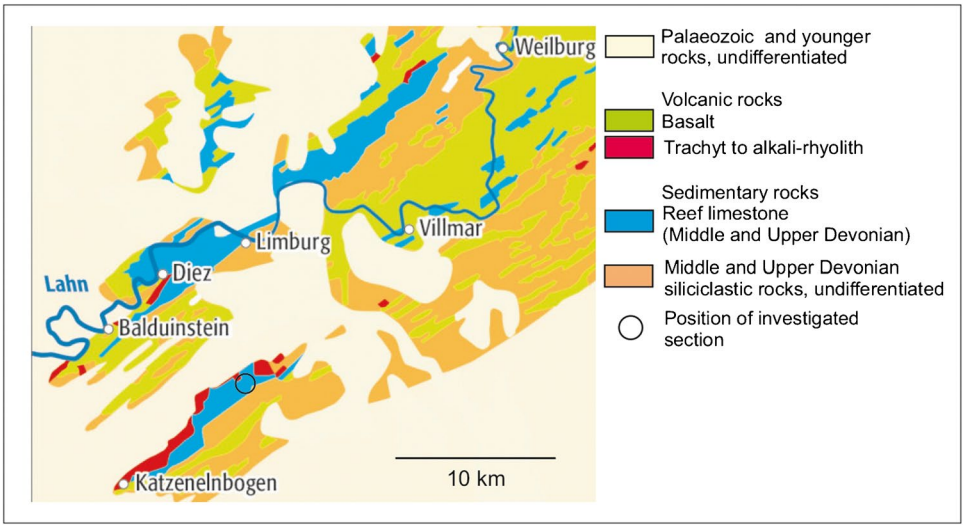

Fig. 2 Simplified geological map of the southwestern Lahn Syncline (partly reproduced from Flick and Nesbor 2021 (Fig. 3.3.1) and location of investigated section)

thin sections of 7.5 x 11 cm in size were used. Microphotographs were taken using a Zeiss Discovery V20 stereoscopic microscope and a Canon EOS body with transmitted light and using 24–85 mm and 100 mm macro lenses. Core photography was performed with a book2net A1. Characterisation of facies types (FT) is based on Facies Zones (FZ) after Embry and Klovan (1971), Standard Microfacies Types (SMF) after Flügel (2004), and are compared with other descriptions and facies models such as Wright (1992) and MacNeil and Jones (2016). Thin sections are stored at the Senckenberg Research Institute and Natural History Museum Frankfurt, Germany, under repository numbers SMF 99299 to 93358. Core descriptions were utilised to determine lithofacies of the deposits and microfacies analysis were then used to determine environmental settings and reef evolution at time of deposition. For geochemical analyses the core was subdivided in 46 sections based on lithological differences. In most cases, 2-4 metres of the core were sampled for geochemical analysis. Sampled intervals do not necessarily correspond to samples taken for facies analysis as facies types are a result of both, polished slabs and thin sections and the detailed description was done in a second step. About a quarter of the core material was crushed in the jaw crusher and about 100 g of the crushed material was ground in the centrifugal mill. Quantitative XRF analyses followed DIN EN ISO 12677. They were carried out at SCHAEFER KALK central laboratory using glass disks prepared by borate fusion and the wavelength-dispersive X-ray fluorescence spectrometer Axios mAX Malvern Panalytical with an x-ray tube power of 3kW. Additionally, carbonate samples were dissolved for conodont biostratigraphy according the standard preparation method described for instance in Ta et al. (2022). Middle Devonian conodont stratigraphy was used according to the new conodont zonation summarised in Fig. 1 of Becker et al. (2016b).

Results

Regional geological setting and age

The investigated section is located in the southeastern Rhenish Massif close to Hahnstätten, approximately 11 km south of the town Limburg. Structurally, this area belongs to the southwestern part of the Lahn Syncline (Fig. 2). The entire area is characterised by imbricated structures and thrusts. The sampled section belongs to the Mudershausen Formation, which has a thickness of 750–1000 m (Nesbor 1984). This formation is mainly composed of reef carbonates, type-localities are the quarries at Hahnstätten (Kalkwerk "Schaefer") and a quarry close to the village of Mudersbach (Requadt 2008). The entire core material is composed of shallow-water reef limestones of different lithology and assigned to the Mudershausen Formation, which is conformably underlain by the Steinkopf Formation and overlain by the Hahnstätten Formation. According to Requadt (2008) the Mudershausen Formation has a stratigraphical range from the Givetian to the Frasnian, based on conodonts and brachiopods.

Rare, well preserved conodonts were found in the succession. Conodonts show a conodont colour alteration (CAI; Epstein et al. 1977) of CAI 4.5 to 5 representing average high CAI values of Devonian conodonts in the southeastern Rhenish Massif (Königshof 2003). Some specimens are slightly deformed and/or are covered by dolomite crystals (Fig. 3). Long-ranging taxa such as *Polygnathus linguiformis linguiformis* and some incomplete shallow-water taxa such as *Icriodus* or *Belodella* species and polygnathid ramiforms were found in two samples only which seems to be a result of limited sample sizes (below 1 kg). In sample HST-79/1 (core 45) we found *Polygnathus linguiformis linguiformis* and *Icriodus regularicrescens* along with some ramiform elements. Whereas *Polygnathus linguiformis linguiformis* has a rather long stratigraphical range, *Icriodus*

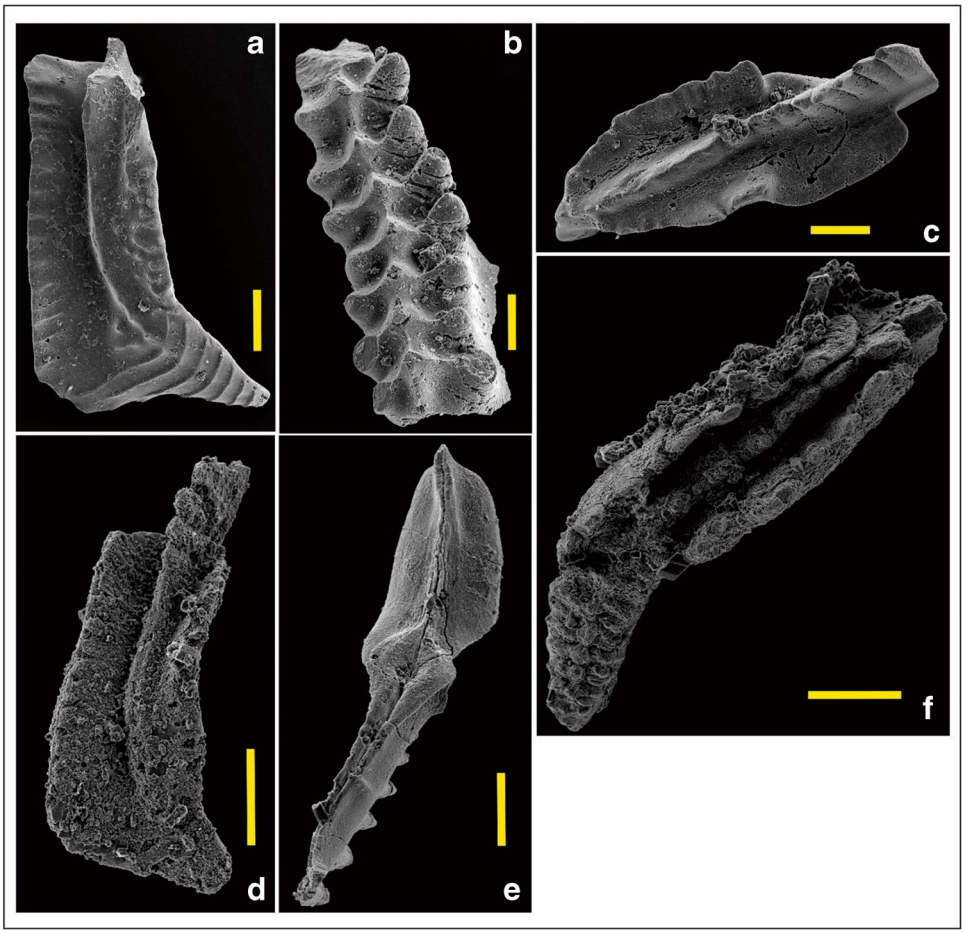

Fig. 3 Important conodonts found in the core: **a** *Polygnathus linguiformis linguiformis* Hinde, 1879, upper view, scale bar = 200 µm (sample HST 79/1); **b** *Icriodus regularicrescens* Bultynck, 1970, upper view, scale bar = 100 µm (sample HST 79/1); **c** *Polygnathus* cf. *ansatus* Ziegler, Klapper and Johnson, 1976, upper view, scale bar = 100 µm (sample HST 79/4); **d** *Polygnathus linguiformis linguiformis* Hinde, 1879 (slightly deformed), upper view, scale bar = 200 µm (sample HST 79/4); **e** *Polygnathus rhenanus* Klapper, Philip and Jackson, 1970, lower view, scale bar = 100 µm (sample HST 79/4); **f** *Polygnathus linguiformis mucronatus* Wittekindt, 1966 (slightly deformed); upper view, scale bar = 200 µm (sample HST 79/4)

regularicrescens last records occur within the lower part of the *Polygnathus rhenanus/varcus* Zone. Thus, this sample most likely represents the Givetian *Polygnathus rhenanus/varcus* Zone. In core 23, sample HST-79/4, we found *Polygnathus linguiformis linguiformis, Polygnathus rhenanus, Polygnathus* cf. *ansatus,* and *Polygnathus linguiformis mucronatus* accompanied by some ramiform elements. *Polygnathus rhenanus* has a stratigraphical range from the *Polygnathus rhenanus/varcus* Zone to the upper part of the *Polygnathus ansatus* Zone (Bultynck 1987). Together with a questionable *Polygnathus ansatus*, which defines the base of the *Polygnathus ansatus* Zone, and the occurrence of *Polygnathus linguiformis mucronatus* (Fig. 3), which is recorded from the *ansatus* Zone elsewhere (Liao and Valenzuela-Rios 2008; Narkiewicz and Königshof 2018) a middle Givetian age for this sample (*Polygnathus ansatus* Zone) is likely.

The biostratigraphic result based on conodonts for both samples is also confirmed by the occurrence of *Stringocephalus burtini*, a classical index fossil of the Givetian stage, which was found in many layers of the investigated section (see lithological log). Holocene sediments have a thickness of about 35 m. The entire core material is composed of shallow-water reef limestones of different lithology. Intensive karstification of Paleogene/Neogene age (Eisenlohr 1983) resulted in hiatuses.

Lithological description and microfacies analysis

The described lithofacies (FTs – see Table 2) shown in Figs. 4, 5, 6, 7, 8, 9, 10, 11 and 12 are not exclusive and transitions between different lithofacies exist. The shown examples represent characteristic facies types, which are most frequent in the entire core. Core number and sample depth (e.g. 10/40.90 – 41.00) is generally shown in each figure, otherwise it is given in the figure explanation. The dominance of reef organisms is represented by corals (mainly *Thamnopora*, alveolitids and rare dendroid rugose corals) and stromatoporoids (e.g. laminar and tabular, dendroid stromatoporoid *Stachyodes*, and bulbous such as *Actinostroma* and *Stromatopora*), which occur with rare bryozoans, algae, and very rare crinoids. Other bioclasts are brachiopods (very frequent is *Stringocephalus burtini*), gastropods, ostracods, echinoderms, rare trilobites, and conodonts. Lithofacies/microfacies analysis interpreted from cores and thin sections in this study indicate different settings ranging from restricted lagoonal to open marine. The majority of these lithofacies are lime mudstone, fenestral microbialites, floatstone, rudstone, and grainstone. In the following sections characteristic lithofacies are described. Palaeokarst of Paleogene/Neogene

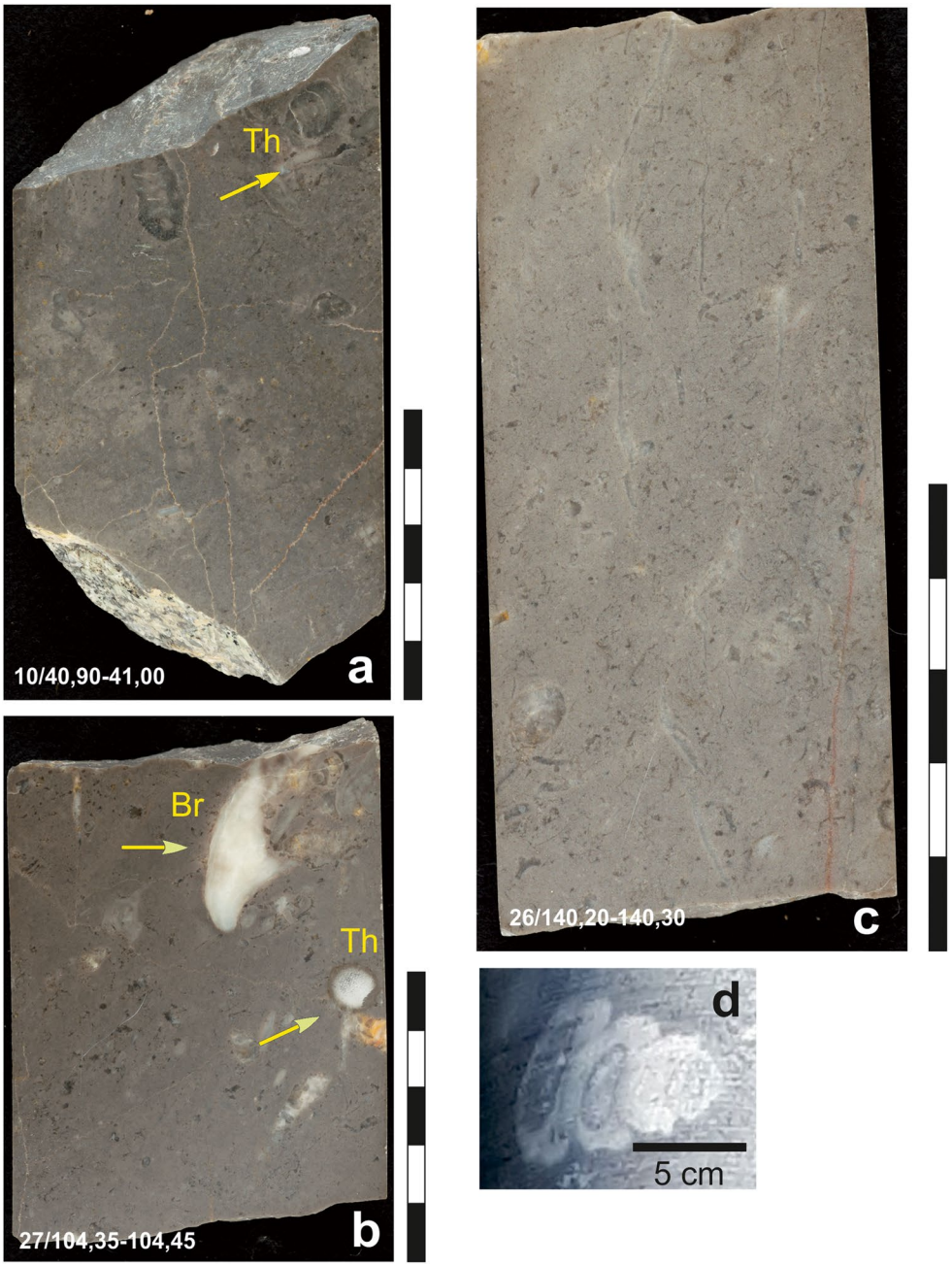

Fig. 4 **a, b** Lime mudstone with rare birdseyes and rare fossils from different depth (*Th* *Thamnopora*, *Br* Brachiopod remnant; scale 5 cm, depth as indicated); **c** lime mudstone with non-oriented isometric and elongated birdseyes at the base. Pelmicritic matrix, very rare bioclasts mainly small shells (scale 5 cm, depth as indicated); **d** large spirally ribbed, pleurotomariid gastropod, sample depth at 39,80 m

age is a common feature in Middle Devonian reef limestones and occurs in some horizons. Fissures are filled with reddish lime mudstone from overlying successions. Synsedimentary fissures occur as well, which exhibit fossil fragments of surrounding sediments.

Lime mudstone lithofacies (FT-1; Figs. 4, 5 and table 2)

Description This lithofacies is characterised by prominently grey, often mottled limestone with few bioclasts (Figs. 4a, b, c). Nodular lime mudstone lithofacies occurs only in a few thin layers and is also characterised by scarcity of biota. Fossil elements include brachiopods such as *Stringocephalus burtini*, as well as rare corals, foraminifera, ostracods, and gastropods (mostly complete). The latter ones can reach remarkable sizes and represent in most cases large spirally ribbed, pleurotomariid gastropods (Fig. 4d). Laminations and bioturbation are preserved in some parts of the succession, whereas fenestral pores of different sizes occur most frequently. Three litho-subfacies can be distinguished, an irregularly laminated fenestral limestone (Fig. 4c) and a regularly laminated fenestral limestone (Figs. 5a, c) with rare fossils, such as foraminifera and ostracods (Fig. 5b), and a bindstone showing relicts of microbial and algal filaments.

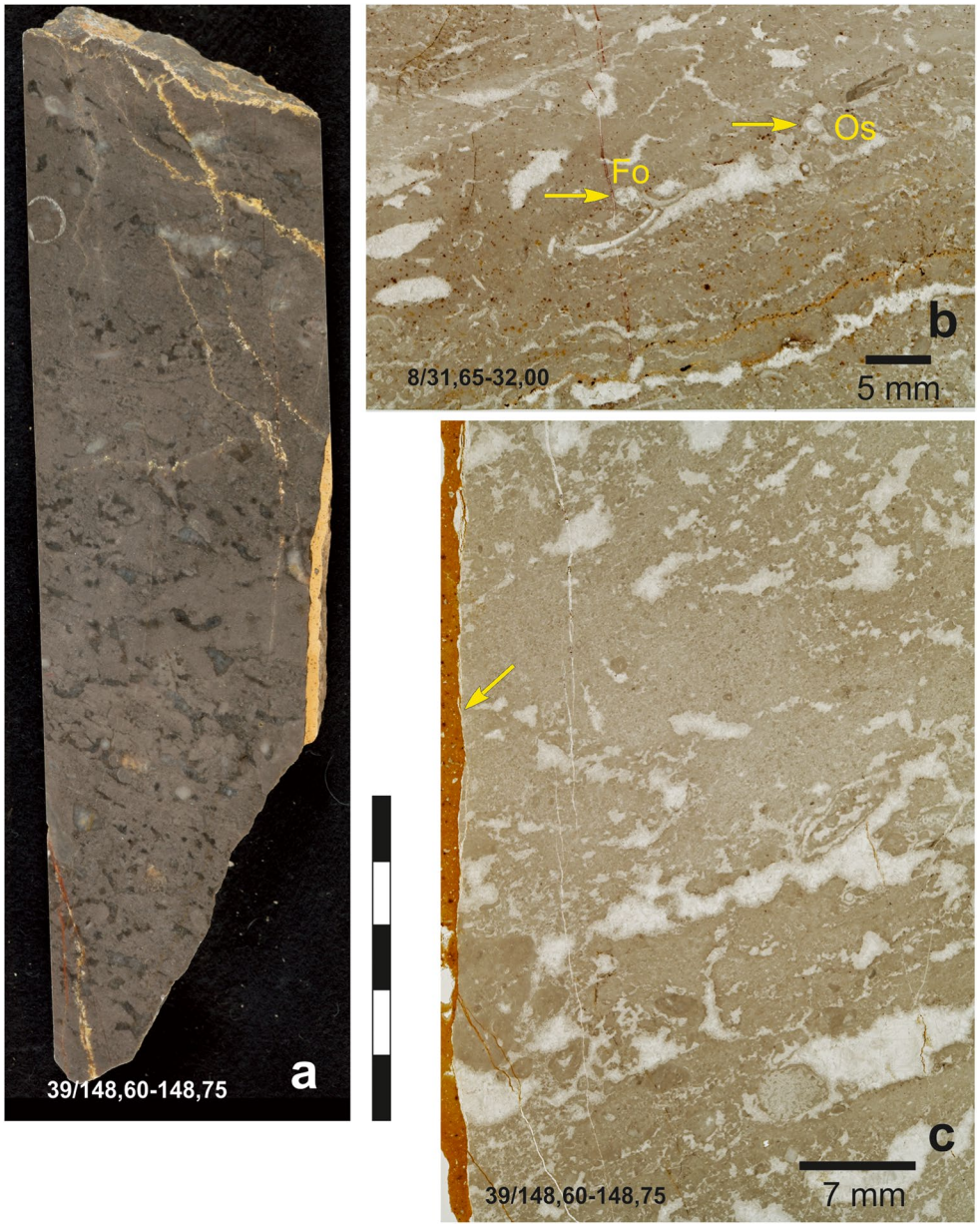

Fig. 5 **a** Lime mudstone with birdseyes, more laminated in the lower part (scale 5 cm, depth as indicated); **b** alternation of peloidal layers and birdseyes layers with rare fossils (*FO* paratheraminiid foraminifera, *OS* ostracod; depth as indicated); **c** detail of laminated fenestral bindstone (lower part of Fig. 4a) with alternating peloidal layers. Birdseyes of different sizes within a peloidal grainstone matrix. Some birdseyes exhibit filling with dark micrite at the base and contain an *Amphipora* branch (lower right side above scale). Left side: vertical palaeokarst fissures filled with reddish lime mudstone (depth as indicated)

The texture is characterised by alternating peloidal layers, micritic layers, and intercalated horizontally elongated, laminate fenestral pores, some of them were filled with micrite at the base (Fig. 5c). Small micrite grains are well rounded, which are grain-supported (rare) or mud-supported. Fenestrae exhibit an irregular shape, which indicates the soft consistence of the sediment.

As a sublithofacies, bindstones occur but they are less frequent. The binding effect of the bindstone lithofacies was enhanced by synsedimentary cementation of intergranular pores. Some samples of this lithofacies show palaeokarst fissures, which are filled with reddish lime mudstone (Fig. 5c) and small limestone clasts. Cracks along fissures exhibit meteoric-phreatic cements.

Interpretation The abundance of lime mud with planar fabric indicates low-energy environment. The presence of fenestral fabric supports the assumption of a microbial community, as microbial layers are characterised by early-cemented micrite with fenestral pores (Pratt 2011). This lithofacies type indicate intertidal, lagoonal facies settings, consistent with interpretations by Whalen et al. (2002), DaSilva and Boulvain (2004) Fåhræus et al. (1974) and others who described similar successions (e.g. Krebs 1974; Koch-Früchtl and Früchtl 1993; Flügel 2004). Peloidal intercalations are interpreted to be a result of clotted micrite, which has been reworked by currents. The overall scarcity of marine biota (e.g. minor *Thamnopora*) is thought to be an indicator of restricted setting (Whalen et al. 2002). Alternation of fenestral and

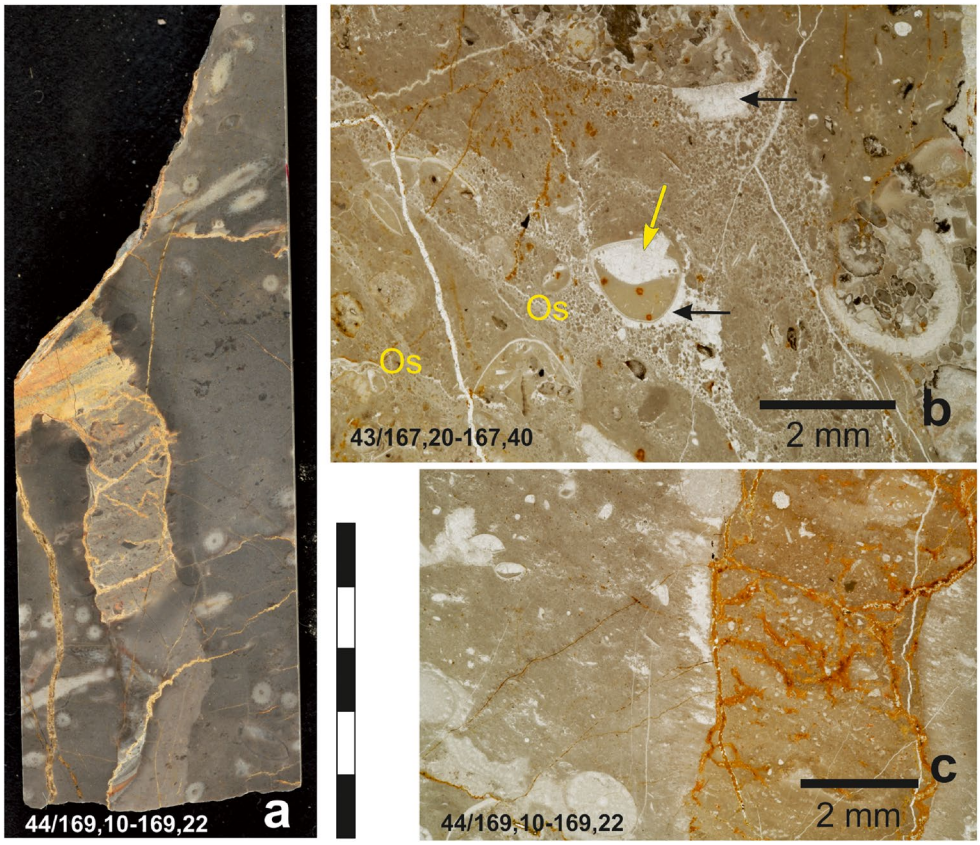

Fig. 6 **a** Lime mudstone to wackestone with corals, shell fragments, and ostracods. Vertical fissure in the middle part (scale 5 cm, depth as indicated). **b** peloidal and bioclastic wackestone with fossils, such as ostracods (OS), brachiopod, and coral fragments. Different cements occur in the geopetal structure and around the shell: the calcite cement of the filling consists of equidimensional small crystals (yellow arrow), whereas the cement around the shell is composed of large crystals (radiaxial fibrous cement), which have a length/width ratio of approximately 1:3 (black arrow); burrowing is common (upper right side, depth as indicated). **c** detail of figure a with *Amphipora*, ostracods, and undifferentiated bioclasts. The fissure is filled with reddish lime mudstone and limestone clasts (upper part). The small-sized bioclasts are mainly composed of shell hash and very rare crinoid ossicles and sponge spicules (depth as indicated)

peloidal fabrics is a characteristic feature of mudmounds and reef lagoons, which were described from other sections in the Rhenish Massif (e.g. Krebs 1974; Mestermann 1995; Stichling et al. 2022) and which is similar to descriptions sensu Flügel (2004; SMF 21), Wilson (1975; FZ 8), Schudack (1993; laminate facies), and Garland et al. (1996; MF9), all pointing to restricted, shallow subtidal, intertidal to supratidal palaeoenvironments. Palaeokarst fissures point to rather supratidal settings. In areas with an absence of fenestral pores the environmental settings are thought to be subtidal, which is supported by the occurrence of ostracods, gastropods, and brachiopods.

Wackestone lithofacies (FT-3; Fig. 6 and table 2)

Description This lithofacies type is rather rare in the entire core. The generally grey, fine-grained limestone contains some corals, such as thamnoporids, alveolitids and ostracods, small gastropods, and brachiopods (Fig. 6a). This limestone shows bioturbation and a variable amount of peloids (Fig. 6b). In some parts the transition to laminated lime mudstone lithofacies is visible. Geopetal structures occur very frequently. The pore-filling is mainly characterised by equidimensional small crystals, whereas the cement around bioclasts is composed of radiaxial fibrous calcite (Fig. 6b). Generally, the bioclastic wackestone is strongly burrowed. This lithofacies also contains some karst-fissures (Fig. 6a, c). The filling is composed of reddish lime mudstone and angular to subrounded limestones clasts. Bioclasts are represented by small shell hash (mainly brachiopod shells), some corals, and ostracods.

Interpretation The overall fine-grained matrix, bioturbation and the fossil content point to deposition below the fair-weather wave base (drowned back reef or within deeper parts of the reef-frame or fore-reef settings). Slow sedimentation rates in low-energy environments (e.g. Stearn et al. 1999; Stearn 2016) is associated with bioturbation. Similar

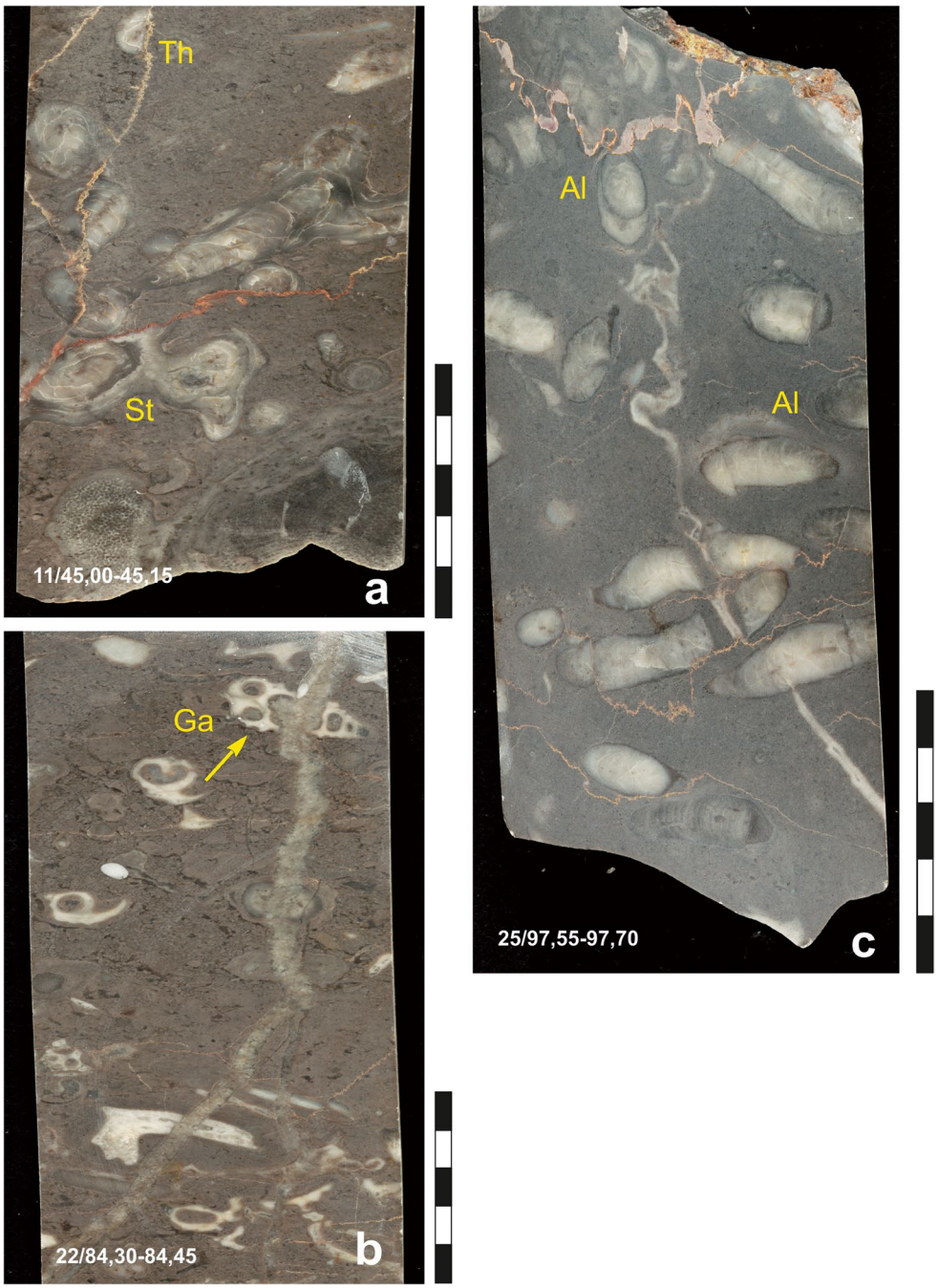

Fig. 7 **a** Stromatoporoid/coral floatstone (scale 5 cm, depth as indicated); **b** gastropod floatstone with large gastropods (scale 5 cm, depth as indicated), both examples show a micritic/peloidal matrix; **c** Coral floatstone in a micritic matrix (*Al Alveolites* sp., depth as indicated)

sediments were described from other reef limestones of the Rhenish Massif by Koch-Früchtl and Früchtl (1993) as "microbioclastic-peloidal wackestone with packstone parts" or very recently by Stichling et al. (2022) as "peloidal and bioclastic mud-wackestone (with reefal debris)". The lack of microbial fabric in the lithofacies of these rocks suggests an oligotrophic environment (MacNeil and Jones 2016). Described cements occur in meteoric-vadose, marine-phreatic and in burial environments (Flügel 2004). The occurring fissures may be explained by submarine fillings as a result of synsedimentary tectonics in a highly mobile setting with coeval volcanic activity or differential compaction. The overall facies points to shallow lagoonal facies with open water circulation, which is consistent to SMF 9 (Flügel 2004).

Floatstone lithofacies (FT-4; Fig. 7 and table 2)

Description The floatstone lithofacies occurs frequently in the core and displays a variety of bioclasts, such as coral/stromatoporoid floatstone (Fig. 7a), gastropod floatstone (Fig. 7b), and coral floatstone (Fig. 7c).

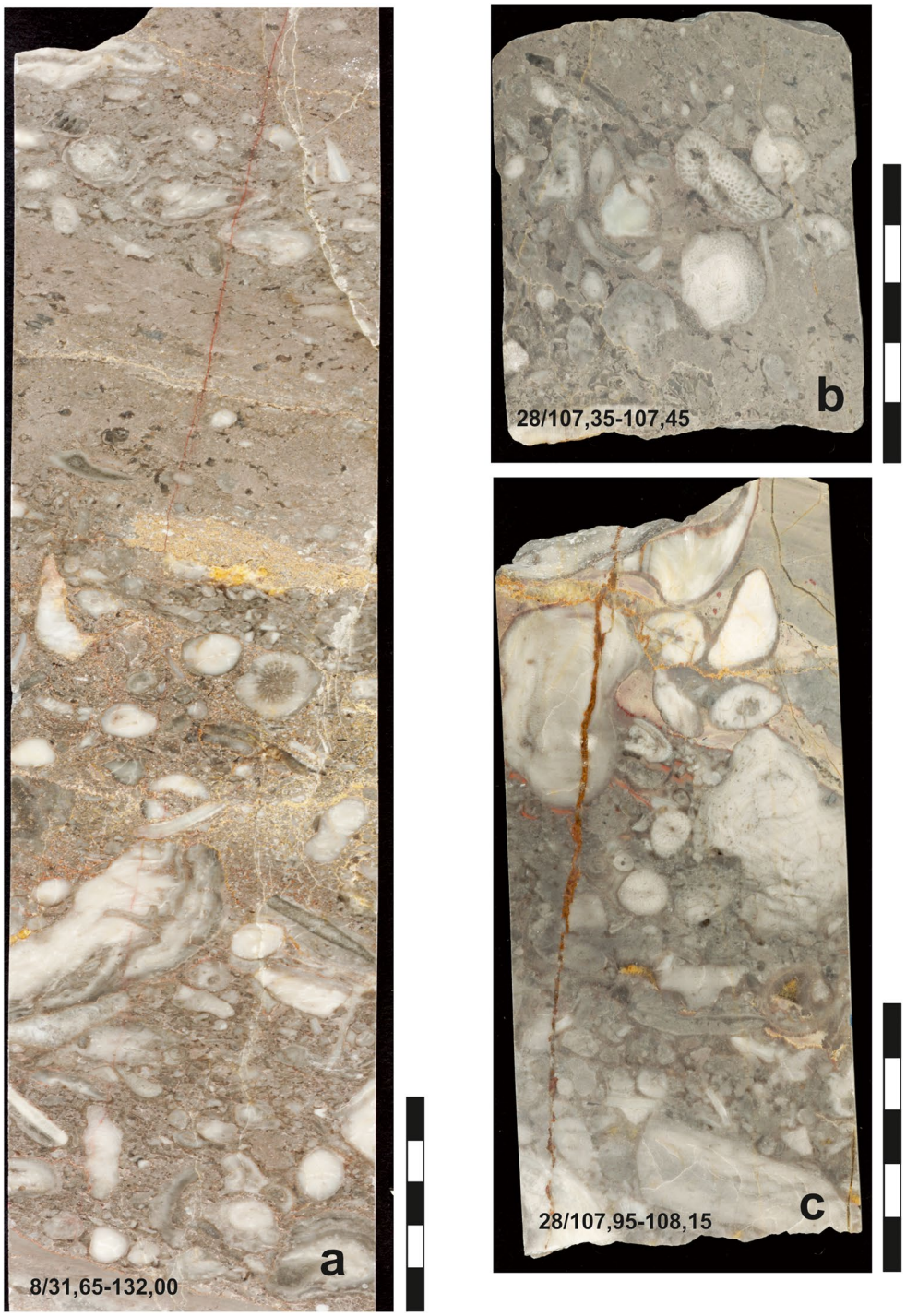

Fig. 8 **a** Coral/stromatoporoid rudstone with lime mudstone intercalation (with rare isometric and elongated birdseyes; scale of all figures 5 cm, depth as indicated); **b** coral/stromatoporoid rudstone/floatstone lithofacies, matrix is a pelmicrite (depth as indicated); **c** poorly sorted rudstone which is overlain by floatstone lithofacies (depth as indicated)

In the coral/stromatoporoid floatstone *Alveolites*, *Thamnopora*, and stromatoporoids (*Stachyodes*) are the main grain types, which are sometimes preserved in life position. Stromatoporoids exhibit laminar and tabulate habitus. The coral floatstone is rather exclusively composed of *Alveolites* and very rare stromatoporoids, whereas the gastropod floatstone contains mainly large spirally ribbed, pleurotomariid gastropods. Corals, brachiopods, and stromatoporoids are very rare. The matrix of each sublithofacies consists of a dark-grey, organic-rich lime mudstone to mottled brown wackestone. In contrast to the first two sublithofacies, the coral floatstone exhibits very few peloids. The overall rare bioclasts of the micritic matrix are composed of brachiopod shells, small ostracods, and gastropod fragments.

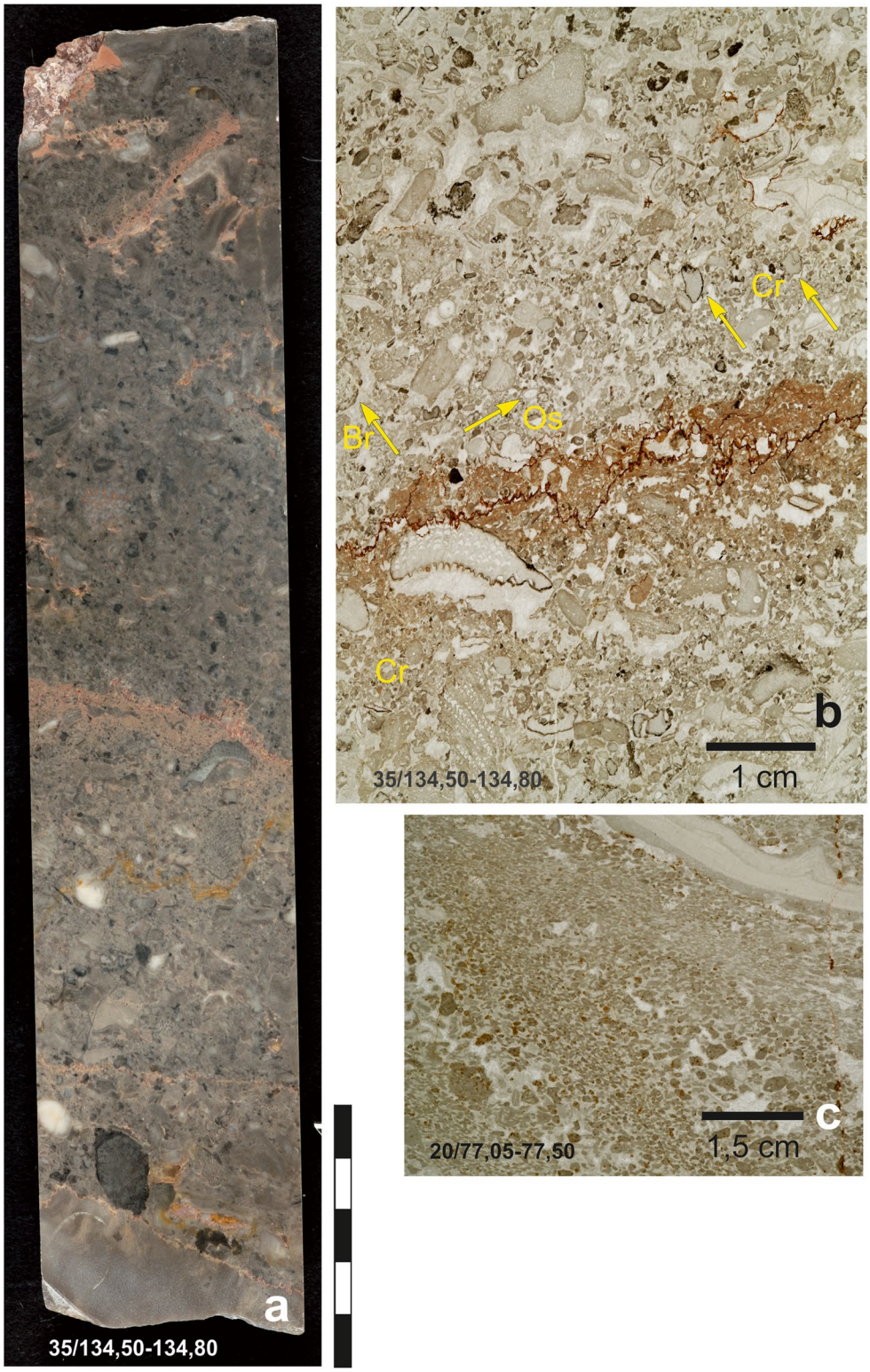

Fig. 9 **a** Characteristic poorly sorted grainstone lithofacies (scale 5 cm); **b** detail of "a" with coated grains, various fossils (*Br* bryozoans; *OS* ostracods; *Cr* crinoids among others), and high amplitude stylolites in the middle part; **c** peloidal grainstone with angular and rounded micritic clasts; a large shell fragment of *Stringocephalus burtini* in the upper right (depth as indicated)

Interpretation The dark-grey, organic-rich coral/stromatoporoid- and coral floatstone suggest small-scaled ecological differences or different sources and have been deposited in back reef palaeoenvironments. The gastropod floatstone represents a sub-lithofacies providing favourable conditions for this group, which is proven by the sizes and numbers of the gastropods in specific samples. The environment is consistent with low-energy levels, reflected in lime-mudstone to wackestone matrices. Gastropod-rich floatstone are well known and have been described as typical back-reef facies

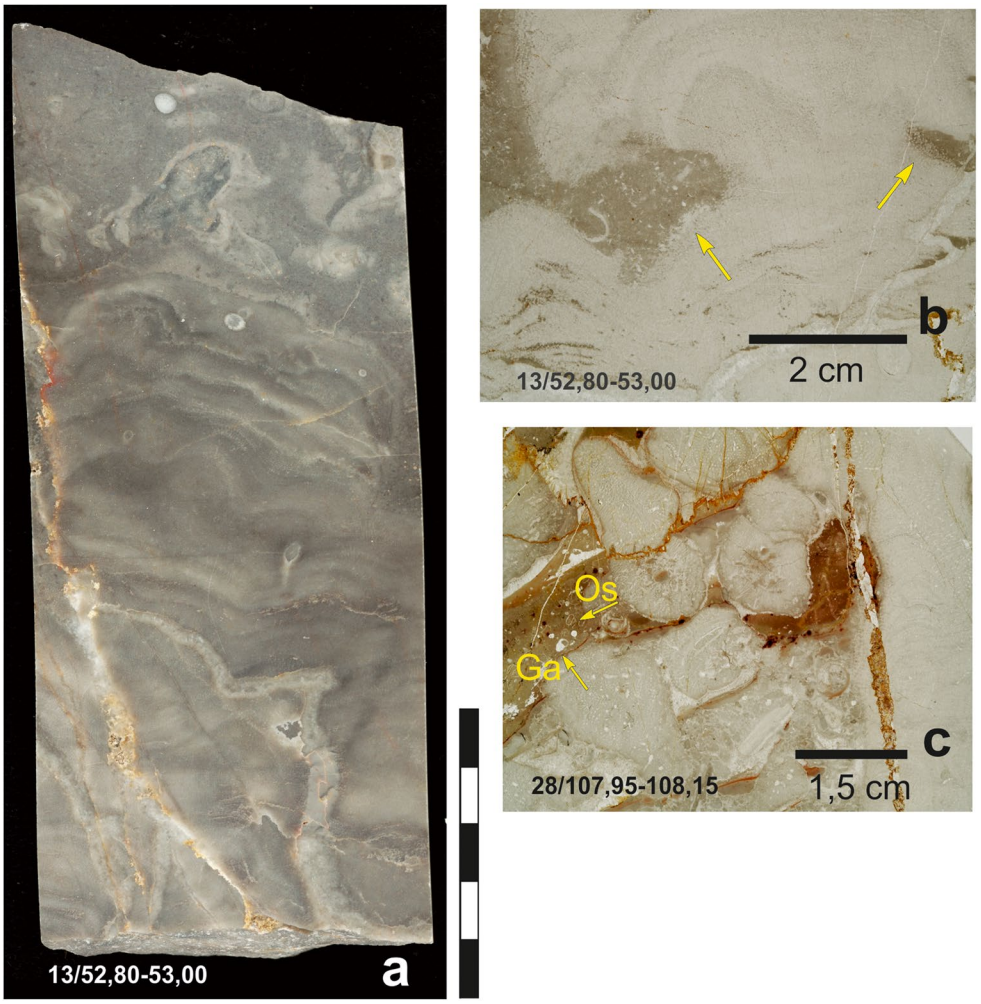

Fig. 10 **a** Stromatoporoid bafflestone covered by lime mudstone (scale 5 cm, depth as indicated); **b** bulbous stromatoporoid (*Stromatopora* sp., vertical cut) exhibits ragged growth form (yellow arrows, depth as indicated); **c** coral/stromatoporoid bafflestone (cut obliquely to grows direction). Micritic matrix contains some gastropods (Ga) and ostracods (Os)

usually in more restricted settings (e.g. Malmsheimer et al. 1991; Weller 1991). Although the latter one differs from the previous sublithofacies, it was summarised here, as all sublithofacies described above point to back-reef environments.

Packstone/rudstone lithofacies (FT-5; Fig. 8 and table 2)

Description The texture of this lithofacies can be mainly characterised as densely packed rudstone, but slightly variations to floatstone occur in some successions (Fig. 8a). This lithofacies is also a very frequent one in the section and represents slightly shallower settings as the previous lithofacies. As a result of that reef builders are more abundant and are larger in sizes than in previous lithofacies (Fig. 8a-c). Ossicles and corals particularly *Thamnopora* as well as laminar to tabular stromatoporoids range in articulation from mm-scale up to 4 cm in length and comprise more than 70% of the bioclasts. Subordinate clasts contain brachiopods, gastropods, bryozoans, and rare crinoid ossicles. Except the latter, the clasts range from subangular to well rounded. Cemented lithoclasts also occur and some are biogenically encrusted (Fig. 8b). Generally, the sediments are poorly sorted. Graded bedding was not observed.

Interpretation The presence of *Thamnopora* is consistent with interpretations of high-energy shallow-water environments (Wood 1999; Hofmann and Keller 2006; John 2012). Coarse gravels of biogenic material and lithified sediment derived from top of the reef or flanks as a result of storm events and were than sedimented in low-energy settings within the reef, which is consistent with the lime mud between the clasts. This lithofacies corresponds to SMF 6 (packed reef rudstone) sensu Flügel (2004).

Grainstone lithofacies (FT-6; Fig. 9 and table 2)

Description The first sublithofacies is composed of various bioclasts. In comparison to rudstone lithofacies the clasts are smaller in size and the bioclasts are more diverse. Beside corals and stromatoporoid clasts, the grainstone contains brachiopods, bryozoans, and crinoids. Many skeletal grains

◂ **Fig. 11** Characteristic stromatoporoid framestone lithofacies with large high domical stromatoporoid in situ (scale 25 cm, depth ranging from 95.35 m to 96.00 m). Note that stromatoporoids settled upon lime mud (arrow)

have micritic envelopes or are completely micritized. Rounded intraclasts occur along with peloids. These limestones are generally poorly sorted (Figs. 9a, b). Most space between clasts are filled with marine cement. In those parts were micrite occurs, the fabric shows stylolites and also grain to grain pressure solution occurs (Fig. 9b).

A second grainstone sub-lithofacies, which occurs as thin-bedded intercalations in lime mudstones, shows a completely different bioclast composition. These peloidal grainstones are embedded in a micritic to sparitic matrix (Fig. 9c) and contain very rare fossils mainly ostracods and gastropods, coral- and shell debris occurs as well. Peloidal micritic clasts are angular to rounded. The peloidal grainstones are not laminated.

Interpretation The first sub-lithofacies is very frequent in the succession and known in other reef limestones (e.g. Stichling et al. 2022). The shallow-water environment was suitable for a number of fossils and the sediment was most likely formed under normal marine salinity and a constant wave action at or above fair-weather wave base or between the wave base and the storm wave base (Flügel 2004). The shallow-water, high-energy setting is consistent with the bioclastic coatings, which occur preferentially in shallow-water environments. This lithofacies corresponds to SMF 11 sensu Flügel (2004), whereas the second grainstone sub-lithofacies represents most probably a shallow subtidal environment with moderate water circulation (SMF 16 sensu Flügel 2004). A similar facies type was interpreted by Stichling et al. (2022) as a "drowned variant of the lagoonal" setting of Flügel (2004).

Bafflestone lithofacies (FT-7; Fig. 10 and table 2)

Description This lithofacies is rather limited and occurs only in some parts of the succession, which may also be a result of sampling (core samples might be not large enough and vertical sections exhibit a limited view). The discrimination between different boundstone is based on the growth forms and growth patters (Flügel 2004). The name bafflestone is in the present case justified, as these rocks show characteristic features such as in-situ stalk-shaped fossils (tabulate coral colonies and stromatoporids; Fig. 10a-c), which trapped lime mud during deposition. The fine-grained sediment between the corals and domical stromatoporoids is composed of a micritic matrix and calcareous siltite. The latter one occurs less frequent. One characteristic feature of this lithofacies is the ragged, uneven outline of the stromatoporoid coenosteum, which represents the interplay between stromatoporoid

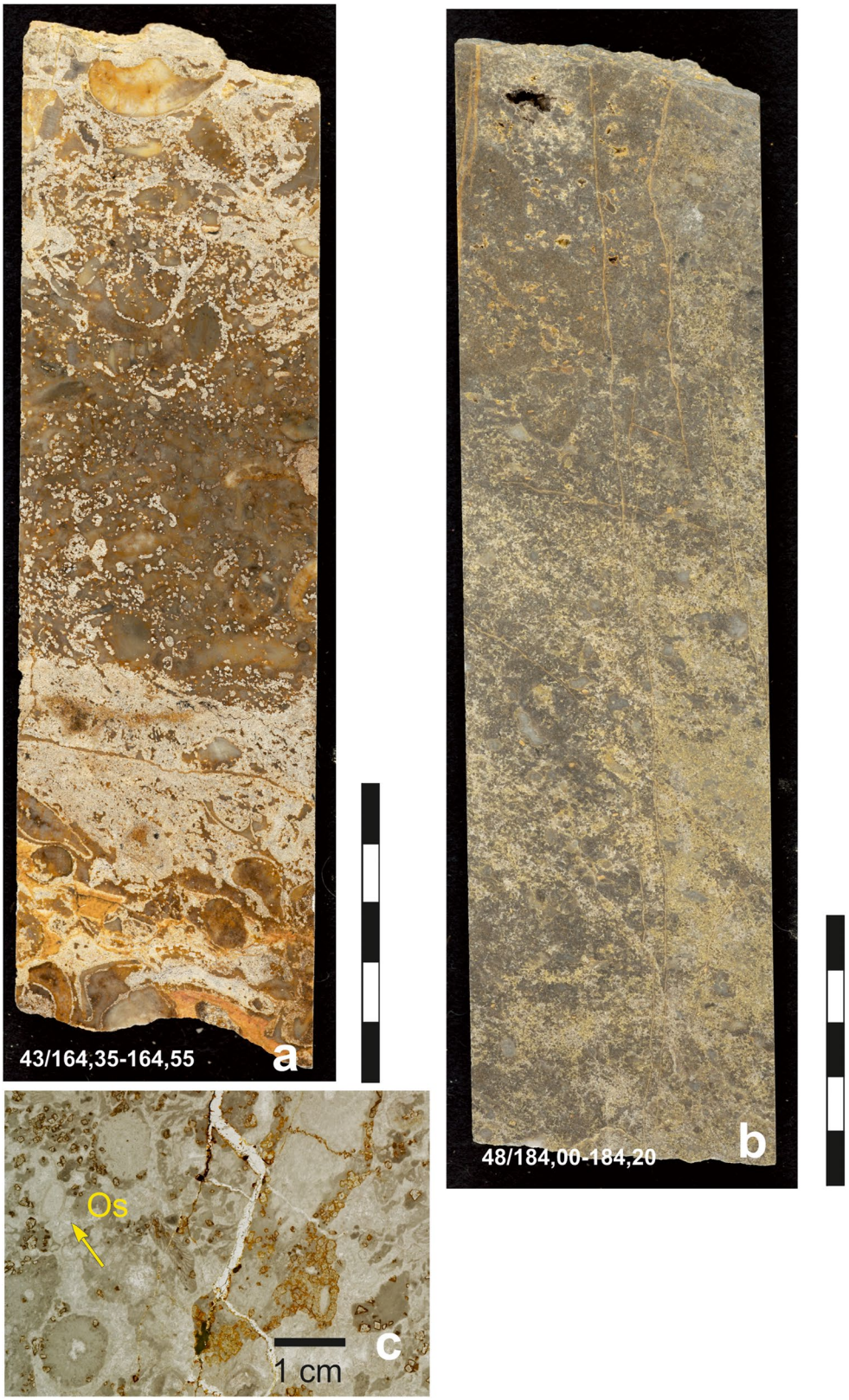

Fig. 12 **a** Heterogenous dolomitization affecting parts of the carbonate rock (rudstone), depth as indicated; **b** obliteration of primary texture of a lime mudstone, depth as indicated; **c** detail of "a"; beginning dolomitization starts preferably within the micritic matrix (euhedral dolomite rhombohedrons) of the rudstone and around the clasts

growth and sedimentation. The first phase is marked by stromatoporoid growth upon a muddy sediment. Sediment accumulation increased and the stromatoporoid became partly covered. In case the stromatoporoid survived as it was not completely covered, it could continue growing upon the sediment (Fig. 10b, c). The repetition of this process led to the

characteristic shape of this morphotype, which is known from many sections elsewhere (Kershaw and Riding 1978; Braun et al. 1994; Königshof and Kershaw 2006).

Interpretation Fossil assemblage, growth form (in-situ stalk-shaped), and internal sediments suggest moderately agitated water conditions in a rather back-reef position, which is consistent with facies zone IV-b of Machel and Hunter (1994) and SMF 7 of Flügel (2004). The occurrence of ragged (Fig. 10b) and mamelon morphotypes of stromatoporoids is a possible indication of rather higher sedimentation rates (Kershaw and Riding 1978).

Framestone lithofacies (FT-8; Fig. 11 and table 2)

Description Another example of autochthonous carbonates occurring in some parts of the section as well, is the stromatoporoid/coral framestone lithofacies. Most stromatoporoids exhibit a domical to high domical habitus, are densely spaced and are preserved in life position. The height of stromatoporoids varies between several centimetres but they can reach more than 60 cm (Fig. 11). Associated with stromatoporids are corals which formed an organic framework that was strengthened by coeval marine cementation. Similar growth forms were described by Königshof et al. (1991) and Braun et al. (1994) from the southern Lahn Syncline and from Morocco (Königshof and Kershaw 2006). Large voids of up to 1 cm between the organic framework were partly filled by marine phreatic, fibrous isopachous cement as well as sparry calcite mosaics.

Interpretation Stromatoporoids found in these autochthonous carbonates can be very large and many authors underline the adaption of growth forms particularly those of stromatoporoids to water energy and thus environmental settings within a reef (e.g. Kershaw and Riding 1978; Riding 1981; Kershaw and Keeling 1994; MacNeil and Jones 2016). The massive morphology of stromatoporoids indicates medium-strength water turbulence (e.g. Machel and Hunter 1994) or rapid growth. But there are a number of other patters which may have influenced biogenic fabrics and growth, such as substrate control and nutrient levels, among others (Wood 1999). The presence of marine cement indicates void space between stromatoporoids and corals and suggests reef-flat environments (Copper 2002a) in higher energy conditions close to the reef front. According to Flügel (2004), these facies correlate to SMF 7 (open marine, marginal reef platform).

Dolostone lithofacies (FT-9; Fig. 12)

Description Dolostone lithofacies is limited to distinct parts and layers in the core. Dolomite cements are so widespread, especially in saccharoid dolomites of lime-mud origin (Choquette and Hiatt 2008 cum lit.). Dolomitisation causes obliteration of primary constituents and texture e.g. bioclastic rudstone (Fig. 12a) or lime mudstone (Fig. 12b). This lithofacies also exhibits selective dolomitization patterns, which is indicated by the dolomitization of fine-grained matrix and/or individual grains (Fig. 12c).

Interpretation Due to the overall shallow-water reefal facies setting and the absence of evaporitic minerals the dolostones may be explained by the seawater dolomitisation models were tidal pumping can be responsible for the formation of dolostones (Carballo et al. 1987). Another way might be thermal convection caused by higher heat flow through a volcanic basement (Aharon et al. 1987). The sediments which were affected by dolomitization are preferably floatstones and lime mudstones, sediments which occur in intertidal and lagoonal facies settings. As the entire reef developed upon volcaniclastic rocks the two options to establish dolostones described above seem likely, beside emersion.

Facies development

The description of facies development of the investigated succession starts from the oldest to youngest part of the core (in order to be consistent with the facies development during deposition). The different reef facies types are summarised in the lithological log (Fig. 13) and are subdivided into 17 depositional units (starting from Unit I to Unit XVII). The majority of lithofacies of these pure carbonates is represented by lime mudstone and fenestral microbialites, whereas bafflestone and framestone are less frequent. Allochthonous carbonates are mainly composed of floatstone, rudstone, and grainstone. Representative thin sections are shown in Figs. 14 and 15.

At the base of the section (200.20 m depth) coral/stromatoporoid bafflestone and framestone occur (Unit I: 200,20 m to 198,00 m depth; Fig. 14a), which are covered by an alternation of floatstone, rudstone, and lime mudstone (Unit II: 198.00 m to 186.00 m). The grain-supported rudstone exhibits reef bioclasts ranging in sizes from 0.3 mm to several cm. Intercalated are lime mudstone with a rare fossil content, some of them are bioturbated. Most frequent are brachiopods such as *Stringocephalus burtini* and ostracods, trilobite remnants are rare. The next unit (Unit III) ranges from about 186.00 m depth to 176.00 m and is composed of an alternation of lime mudstone and floatstone. This unit is mainly covered by lime mudstones and rudstone (Unit IV; 176.00 m to 161.65 m) with intercalations of rare wackestone and floatstone (Fig. 14b). Unit V is mainly composed of grainstone and lime mudstone in the upper part. Well-washed bioclastic grainstone occurs from

161.65 m depth to 158.60 m (Fig. 14c) with an intercalated packstone horizon.

These rocks are overlain by rudstone, lime mudstone (Fig. 14d) with fenestral fabric, and floatstone. Two hiatuses occur above, which are a result of karstification. The overlying unit (Unit VI; 153.50 m depth to 148.50 m) is mainly composed of rudstone, bindstone, and framestone. In some framestone, laminated sediment infillings occur in reef cavities. Reddish lime mudstone exhibits manganese-iron enrichments at the base of each layer (Fig. 14e). The infilling sediment is composed of lime mud with rare ostracods, representing the overlying sediment in the core. This succession is overlain by an alternation of mainly rudstone and lime mudstone (Unit VII; 148.50 m to 129.10 m depth; Fig. 14f), with intercalations of grainstone and rudstone/packstone (unit ranging from 148.50 m depth to 129.10 m). Fenestral fabric in lime mudstone occurs very frequently (Fig. 15a), which suggests tidal to supratidal palaeoenvironments. The very shallow-water setting is also proven by the occurrence of meniscus cement. The former calcite in that case is replaced by dolomite (Fig. 15b).

The following Unit VIII ranging from 129.10 m depth to 117.00 m is dominated by coral/stromatoporoid floatstone and rudstone lithofacies with intercalations of lime mudstone, grainstone, and wackestone in the upper part. The unit above the karst (Unit IX; 113.75 m depth to 102.65 m) exhibits a sedimentary succession of bafflestone, framestone, rudstone, and lime mudstone, which is repeated twice (Fig. 13). In the lime mudstones large brachiopod specimens of *Stringocephalus burtini* occur frequently. Overlying rocks (Unit X ranging from 102.65 m depth to 91.00 m) are composed of coral/stromatoporoid framestone, floatstone, and lime mudstone. Coral/stromatoporoid framestone often contains geopetal structures. The laminated brownish mud was deposited within the reef-frame. In a later stage during diagenesis, the existing space was filled with marine and burial cement (Fig. 15c). A number of framestone exhibit high-domical stromatoporoids of more than 60 cm height (96.00 m to 95.35 m depth, Figs. 11 and 13). Some floatstones show beginning dolomitization (Fig. 15d) around and within bioclasts, preferably in a micritic matrix, similar to those described from deeper parts of the section (see Fig. 12a, b). The next unit (Unit XI; 91.00 m to 83.70 m depth) is composed of grainstone (sub-lithofacies one, Fig. 9b), which is overlain by an alternation of floatstone and rudstone (Unit XII; 83.70 m to 76.45 m depth) containing large brachiopod shells (Fig. 15e). Intercalated in this succession is one grainstone horizon. Unit XIII (76.45 m to 65.00 m) is composed of very shallow-water lime mudstone (partly dolomitized) and fenestral bindstone with some intercalations of floatstone and rudstone. A thin bafflestone horizon represents the beginning of the next unit (Unit XIV; 65.00 m to 61.10 m depth), which mainly contains floatstone beside lime mudstone, whereas bindstone is rare. This part is covered by Unit XV (61.10 m to 50.70 m depth) which records preferably framestone, bindstone, and bafflestone. Lime mudstone and floatstone are less frequent. The next younger succession (Unit XVI; 50.70 m to 38,00 m depth) shows frequent facies changes from rudstone, floatstone (Fig. 15f), lime mudstone, and autochthonous framestone. A characteristic feature of these framestone are the often observed microbial crustation around reef building organisms, which led to stabilisation and preservation of reef structures (Fig. 15g). The matrix exhibits peloidal and clotted structures, which were also reported from other sections, for example from the Harz Mountains (Gischler 1995) and are also well-known from sections in the Rhenish Massif (e.g. Löw et al. 2022; Stichling et al. 2022. The youngest unit (Unit XVII; 38.00 m depth to 31.65 m) represents an overall subtidal to supratidal palaeoenvironment with lime mudstone and fenestral bindstone. Intercalated are rather thin horizons of rudstone (Fig. 15h), grainstone, and floatstone, which are overlain by Holocene sediments (Fig. 13).

Geochemistry

The sedimentological record of the studied section exhibits different lithological/facies differences but all samples represent shallow-water conditions ranging from supratidal, shallow-subtidal to open marine, marginal reef platform environments. Trace element geochemical analysis shows remarkably stable signatures of calcite values. Calcite content of these ultrapure carbonates have values ranging from 81.57vol% to 99vol%, whereas the majority of calcite values is above 98% (Table 1). Those pure limestones are used for different purposes by the company but they are primarily designed to be used in food production, beverage industry and much more. The geochemical analysis focusses on different elements but in respect to palaeoenvironmental settings CaO, Fe_2O_3, MgO, and P are important (Table 1).

The average quality of the limestone samples lies at 97.68% CaO, which means that the majority of the samples represent pure limestones. The extremely high purity of limestones makes it difficult to identify correlations between lithofacies and geochemical differences of the rocks. Furthermore, some samples taken for geochemical analysis overlap different lithofacies as samples were taken prior to the detailed lithological/microfacies description. Nevertheless, some results are obvious. Samples from framestone and bafflestone exhibit a high purity of limestone, whereas other lithofacies types show a mixture of high purity and "impurities" in terms of Si-, Al-, and Fe values. Dolostones generally show high MgO concentrations, which also were recognised in floatstone and rudstone lithofacies. Dolomitization is most

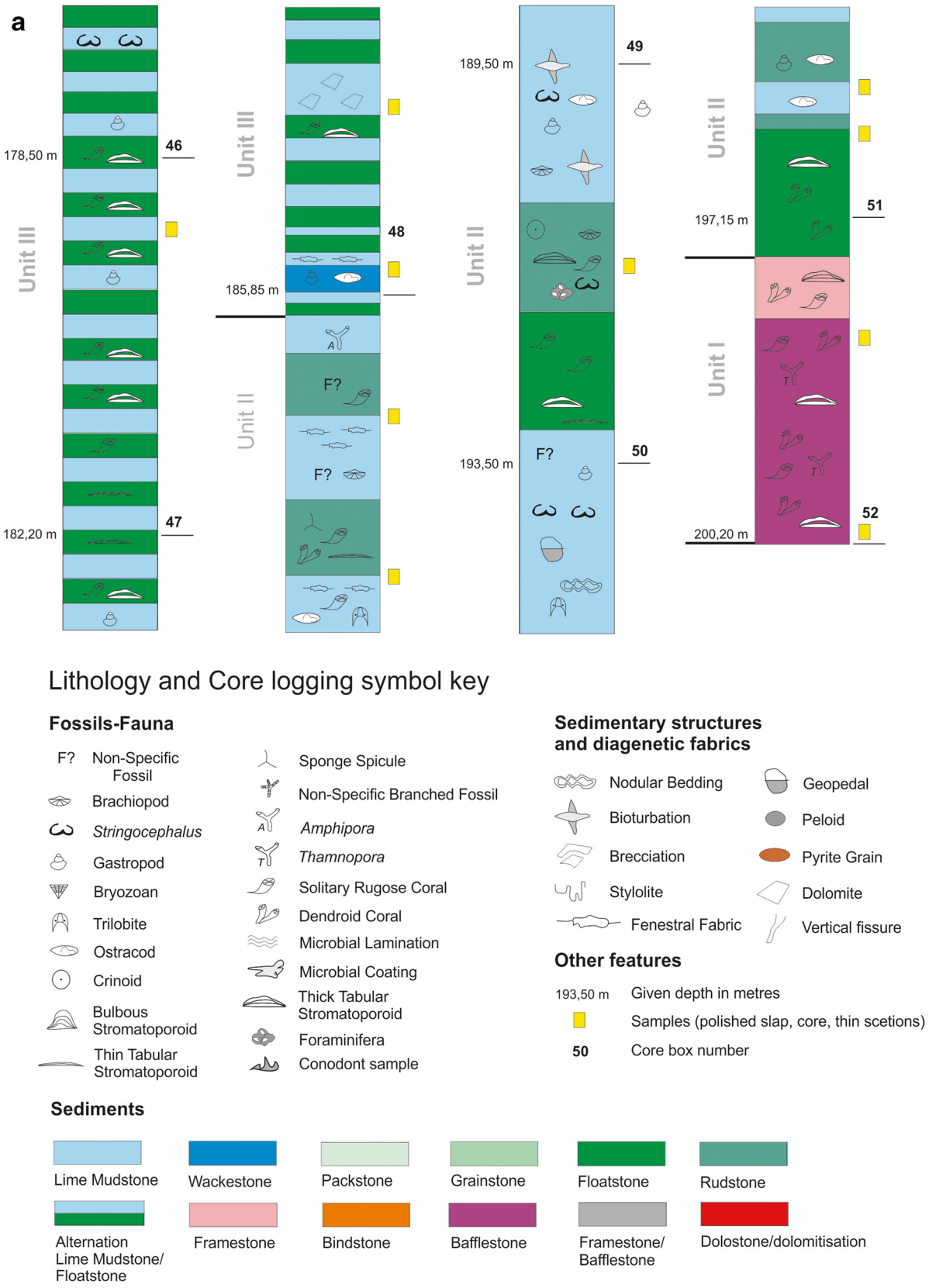

Fig. 13 **a** Lithological log of the section (oldest part; core HST 79) which was subdivided into 17 lithological/facies units. Description always starts from the right column to the left columns (from oldest part to youngest parts; for orientation compare metres in depth). Fig. 13 **b** Lithological log of the section (continuous). Fig. 13 **c** Lithological log of the section (continuous). Fig. 13 **d** Lithological log of the section (youngest part)

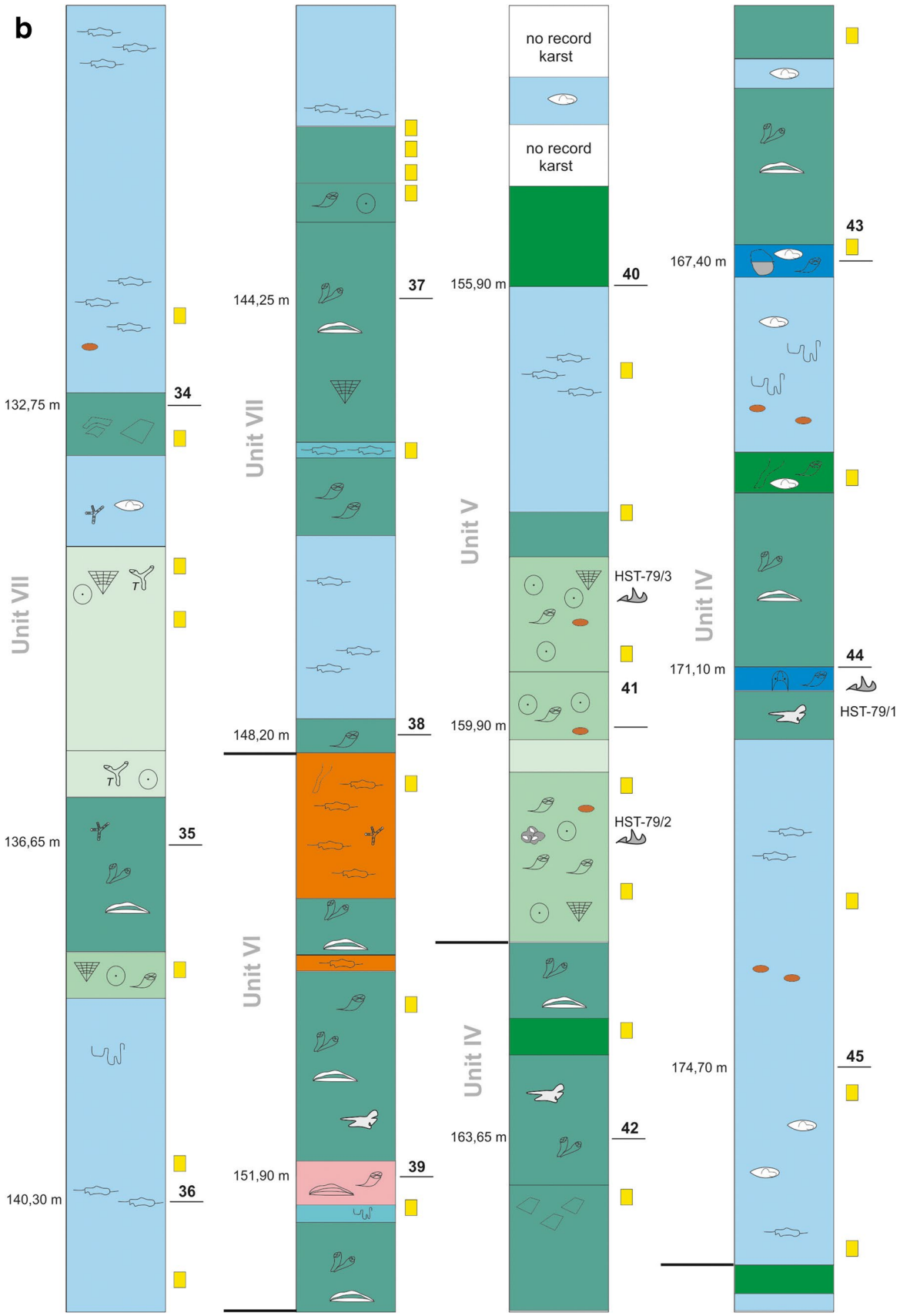

Fig. 13 (continued)

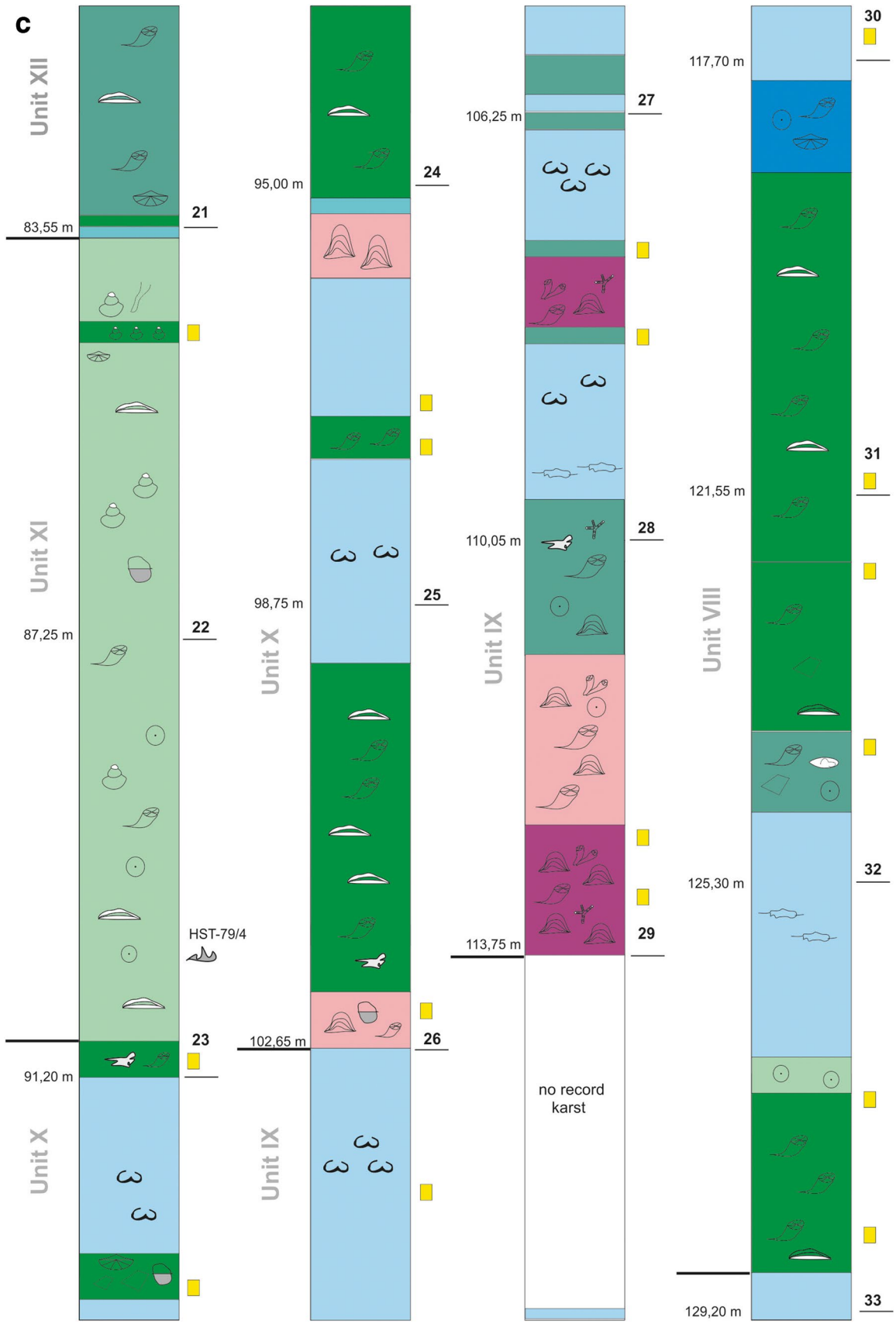

Fig. 13 (continued)

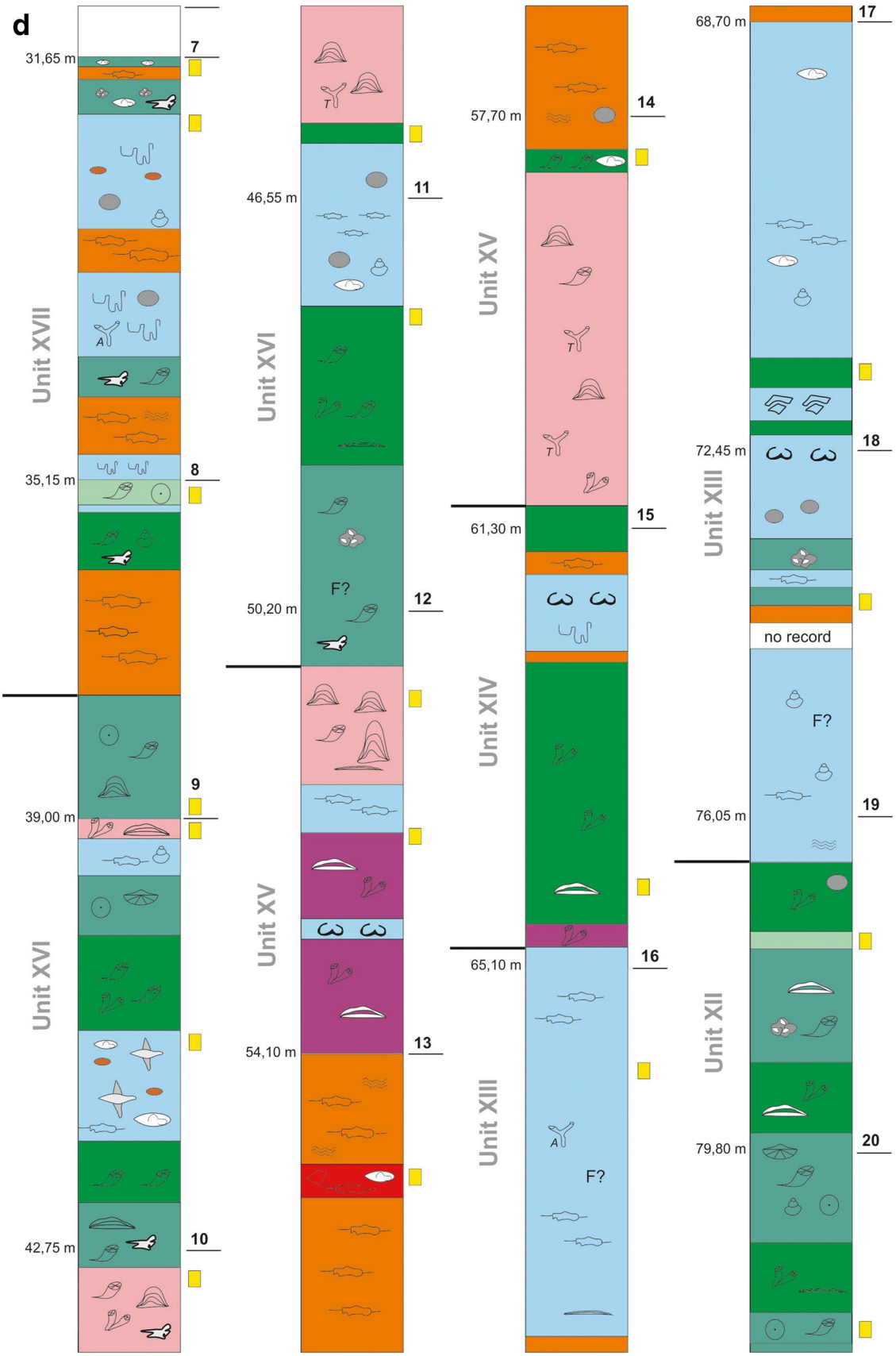

Fig. 13 (continued)

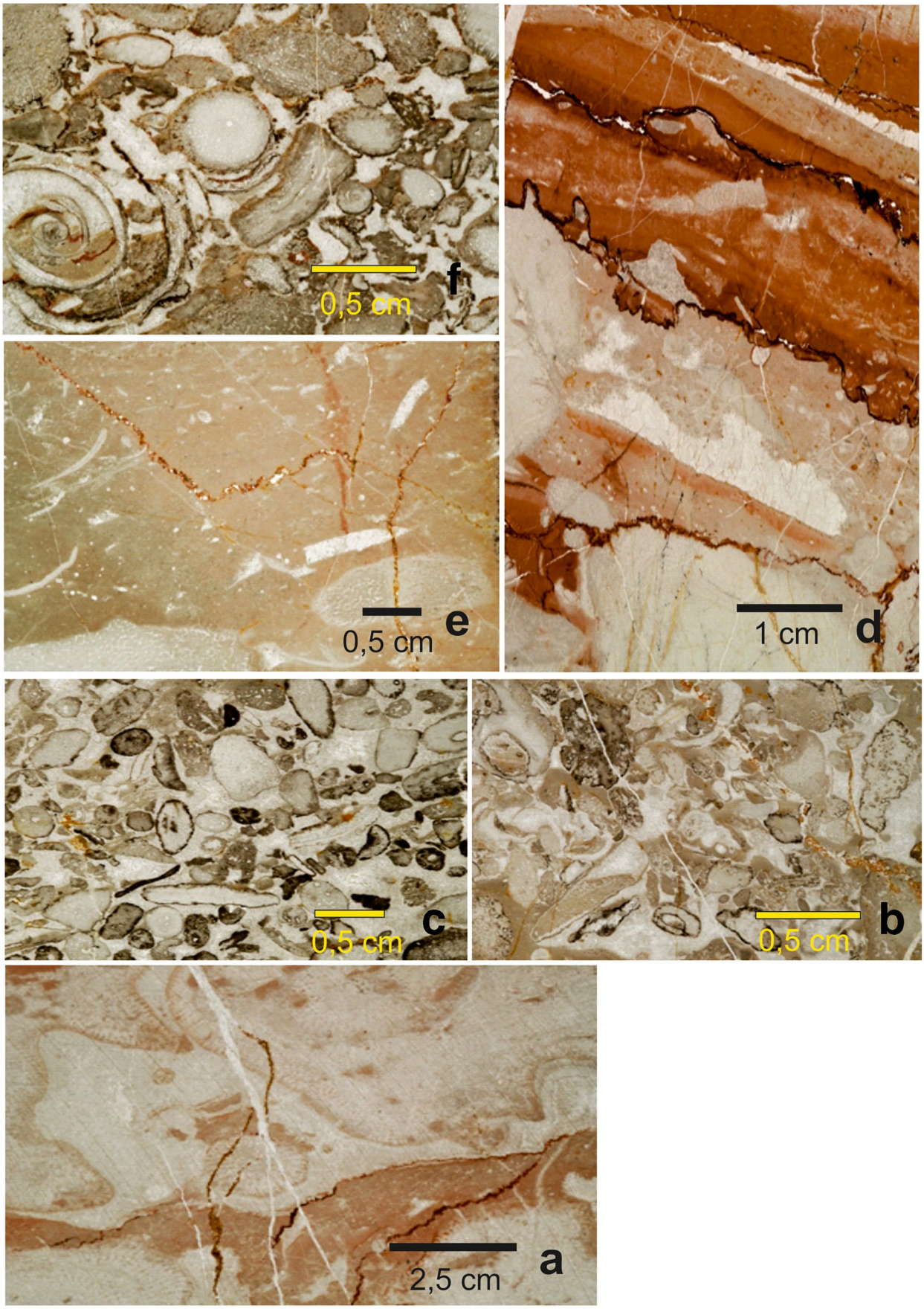
0,5 cm
f
1 cm
d
0,5 cm
e
0,5 cm
c
0,5 cm
b
2,5 cm
a

◂**Fig. 14** Thin sections from different depth (starting from the oldest parts to the youngest to be consistent with facies development during deposition): **a** coral/stromatoporoid bafflestone in a micritic matrix, the coral is overgrown by a stromatoporoid (200.20 to 200.00 m); **b** rudstone/grainstone with partly coated bioclasts; geopetals: complete shells are filled with micrite and marine cement (165.45 m to 165.40 m); **c** well washed bioclastic grainstone with rounded lithoclasts and some coated grains; some particles exhibit iron-manganese rims (160.60 m to 160.35 m); **d** reef cavities: light reddish lime mudstone/wackestone (space is filled by marine phreatic cement) is overlain by dark reddish laminated lime mudstone (152.25 m – 152.20 m); **e** transition from rudstone to lime mudstone/wackestone facies (158.20 m – 158.00 m); **f** poorly sorted bioclastic rudstone; interparticle pores are filled with marine and burial cement; gastropod geopetal at the left (143.80 m to 143.60 m)

frequent in sample 79-36 (Table 1) in a mudstone/floatstone lithofacies with MgO values of 15.28%. Generally, "impurities" occur in deeper parts of the drill core (= older parts), whereas in the upper part of the section pure limestones are more frequent.

Discussion

Reefal carbonates are well known from the southwestern Lahn Syncline, such as from the Villmar Reef, reef limestones from the Kerkerbach Valley, the Balduinstein Reef, and the Hahnstätten Reef (e.g. Oetken 1997; Requadt 2008; Königshof et al. 2010; Königshof and Flick in press, this issue), which have been developed upon pyroclastic deposits (Nesbor 1984; Nesbor et al. 1993). The reef carbonates of the studied section are composed of a mixture of different lithofacies and microfacies types, which overall represent different shallow-water environments, ranging from low-energy lagoonal to subtidal and high-energy reef platform environments (Table 2).

The core does not provide sedimentologic evidence of a slope setting, which would require shelter porosity and graded bedding, among other sedimentological features, but is composed of sediments of back-reef and lagoonal facies. Nine lithofacies types including subfacies types (FTs) are described. The majority of lithofacies of these carbonates is represented by lime mudstone and fenestral microbialites. Birdseyes and laminated-fenestral fabrics occur preferentially in shallow near-coast supratidal and upper intertidal environments. The environments with higher energy are represented by bioclastic rubble deposits, such as rudstone or grainstone (Table 2).

The coral community is dominated by tabulate corals, but also includes solitary and occasionally colonial rugose corals. Tabulate corals most commonly exhibit foliose and massive morphologies, but encrusting and branching growth forms also occur. Stromatoporoids are dominated by *Stachyodes*, *Actinostroma*, and *Stromatopora* species. The depositional environment was characterised by a shallow-water depth and generally low to moderate hydrodynamic energy. High sedimentation rates occur frequently, which is proven by ragged domical growth forms of stromatoporoids (e.g. Fig. 10b). Morphological differences in stromatoporoids such as high-domical, low-domical, tabulate, and laminar growth forms recognised in autochthonous carbonates may be explained by adaption of growth forms to water energy and, thus, environmental settings within a reef (e.g. Kershaw and Riding 1978; Riding 1981; Kershaw and Keeling 1994; MacNeil and Jones 2016). For instance, high domical growth forms, of about 70 cm (see Fig. 11) may indicate medium strength water turbulences or rapid growth, suggesting that the reef development kept up with a sea-level rise or drowning as a result of compaction and/or cooling of the underlaying volcanic body.

The overall diversity of reef-building organisms is rather low. Other bioclasts are brachiopods, gastropods, ostracods, foraminifera, echinoderms, trilobites, and conodonts in descending order. Low diversity communities within a reef may be linked with environmental stress (Flügel 2004), which could be the reason as well in the Hahnstätten Reef. Environmental stress could be related to volcanism, local tectonics, and rapid/frequent local transgressive-regressive cycles. In fact, the entire region was influenced by syn-sedimentary tectonics as a result of extensional tectonics along half-graben structures and volcanism during the Mid-Devonian, particularly in the Givetian (Nesbor et al. 1993; Nesbor 2008; Königshof et al. 2010; Flick and Nesbor 2021). Pulses of sea-level changes are obvious in the investigated section. Evidences of transgressions are documented by bioclastic rubble deposits such as grainstone and rudstone. In both sediments extraclasts were observed. Another indication is the occurrence of suspension feeders (echinoderms) and syntaxial cements enclosing grains in grainstone and packstone. Micrite envelopes caused by microbial microborings and infilling of the holes by micrite (cortoids) were observed in most grainstone (e.g. Fig. 14c). Along with mineralized microbial crusts these are further indications of a transgressional phase (e.g. Flügel 2004). Grainstone and packstone very often overlie lime mudstone and bindstone (Fig. 13). Enrichments of Fe, Mn, and P are common in crusts of drowning carbonates and might be related to higher nutrient content in the water column (e.g. Hallock and Schlager 1986; Föllmi et al. 1994; Drzwiecki and Simo 1997) reflecting changes from oligotroph to eutrophic conditions. Although some geochemical samples overlap different lithofacies and, thus, it is difficult to correlate lithofacies vs. geochemical signals, sample HST 79-36 (rudstone) records remarkably increased Fe_2O_3, Mn_3O_4, and very high MgO values

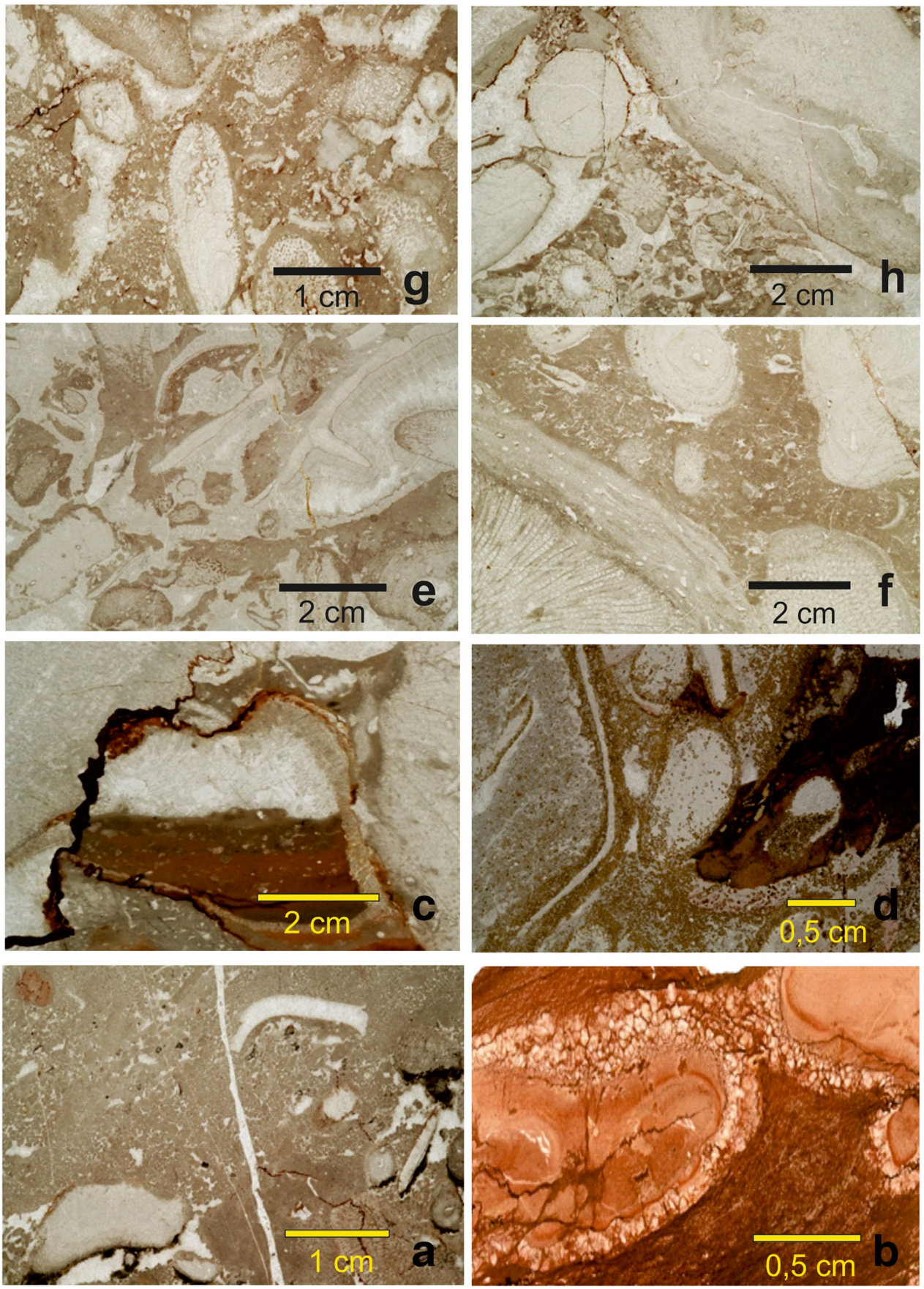
1 cm
g
2 cm
h
2 cm
e
2 cm
f
2 cm
c
0,5 cm
d
1 cm
a
0,5 cm
b

◂**Fig. 15** Thin sections from different depth (description from the oldest to youngest parts to be consistent with facies development during deposition): **a** transition from rudstone to fenestral lime mudstone (142.25 m to 142.15 m); **b** lime mudstone; former calcite cement precipitated in meniscus style was replaced by dolomite; supratidal – intertidal environment (132.36 to 132.25 m); **c** laminated lime mudstone and different cement generations (marine and burial) filled the cavity between bioclasts within a framestone, iron-manganese mineralizations occur at the left side of the cavity (102.30 m to 102.20 m); **d** beginning dolomitization around and between bioclasts of a coral/stromatoporoid floatstone (93.10 m to 92.95 m); **e** coral/stromatoporoid rudstone with a reworked large shell of *Stringocephalus burtini* in a micritic matrix (lime mudstone to wackestone with small ostracods and gastropods); 81.40 m to 81.20 m); **f** coral/stromatoporoid floatstone in a micritic matrix contains some birdeyes (47.75 m to 47.70 m); **g** coral/stromatoporoid framestone; some bioclasts contain microbial crusts, which stabilise and preserve the reef frame (39.20 m to 39.00 m); **h** bioclastic rudstone; interskeletal pores are filled with burial calcite cement (32.00 m to 31.65 m)

in limestones, which are strongly dolomitized (Table 1). A remarkable high P_2O_5 value was found in sample HST 79-16 (grainstone). On the other hand, other grainstone lithofacies exhibit rather low Fe, Mn, and P concentrations. The extremely high purity of limestones makes it difficult to identify correlations between lithofacies and geochemical differences of the rocks but it is obvious that "impurities" of the studied limestones are more frequent in the lower part of the succession, were dolomitization is more abundant as in the upper part. It might be that thermal convection caused by higher heat flow through a volcanic basement (Aharon et al. 1987) led to dolomitization preferably in the lower part of the succession. Dolomitisation in the upper part of the section occurs in some layers, mainly in lime mudstones, which might be a result of tidal pumping (Carballo et al. 1987) or it records a falling stage system tract, which overlies a transgressive system tract, represented by various lithofacies. The latter interpretation might be possible as well, but due to the limited sample size (core samples, there is no lateral correlation to other samples in this report) this remains an assumption.

Based on the conodont record of the succession an age ranging from the *Polygnathus rhenanus/varcus* Zone to the *Polygnathus ansatus* Zone is likely. During this time several sea-level changes took place (Johnson et al. 1985). Abrupt warming in the late Givetian (Van Geldern et al. 2006; Elrick et al. 2009; Joachimski et al. 2009) could be responsible for sea-level rises. The influence of eustatic sea-level change is difficult to estimate, as magnitudes of Palaeozoic sea-level curves are largely unknown (Haq and Schutter 2008). This sea-level curve by Johnson et al. (1985) was later modified by Brett et al. (2011) who recognised a number of minor eustatic transgressions in the Mid-Devonian of eastern North America, which may correspond to sea-level changes observed in the studied section, but this is not sure due to the distance and limited biostratigraphic control. Whether the observed pulses of sea-level changes (e.g. lime mudstone – framestone – rudstone) represent rather local events or eustatic pulses during the Givetian remains questionable and also the scale of sea-level fluctuations seems to be rather small, but possibly sufficient to produce cycles observed in the sedimentological record (Fig. 13). For instance, within core 45 a deepening upward succession was recognised, beginning with lime mudstone, which are overlain by rudstone and wackestone. The latter indicate a lagoonal setting with open water circulation (SMF 9, Flügel 2004), which may represent deposits of a sufficient sea-level rise, which is linked with an eustatic sea-level rise occurring in the *Polygnathus rhenanus/varcus* Zone.

Conclusions

- The core of ultrapure reef limestones of the Hahnstätten Reef exhibits nine different lithofacies/facies types, which mainly represent low-energy, shallow-subtidal, intertidal to supratidal environments.
- Based on the brachiopod *Stringochephalus burtini*, which occurs in the entire succession, and rare conodont samples, the succession has a stratigraphical range from the early middle Givetian (*Polygnathus rhenanus/varcus* Zone to *Polygnathus ansatus* Zone).
- Main reef builders are stromatoporoids and corals. Diversity is low but reef building organisms show a variable morphology, depending on water energy and environmental setting within the reef.
- Sea-level changes are primarily linked to local phenomena, such as synsedimentary tectonics and/or volcanism but eustatic sea-level changes cannot be excluded, particularly during the *Polygnathus rhenanus/varcus* Zone.
- The succession is composed of ultrapure limestones. That makes it difficult to identify correlations between lithofacies and geochemical differences of the rocks. It seems likely that "impurities" of the studied limestones are more frequent in the lower part of the succession, were dolomitization is more abundant as in the upper part.
- Dolomitized limestones might be a result of tidal pumping, thermal convection caused by higher heat flow through a volcanic basement, or even emersion.

Table 1 Geochemical analysis of core HST-79; units 1 – to 17 = same units in figure 13 (lithology). Geochemical samples can overlap different facies types (FTs). Explanations in the text

Sample	Depth from	Depth to	CaO [wt%]	SiO_2 [wt%]	Al_2O_3 [wt%]	Fe_2O_3 [wt%]	MgO [wt%]	Mn_3O_4 [wt%]	SO_3 [wt%]	BaO [wt%]	P_2O_5 [wt%]	Pb [ppm]	Unit	Lithology
79 - 1	31.1	34.8	98.63	0.22	0.13	0.07	0.82	0.02	0.02	0.00	0.03	0.77	17	Mudst. Bindst. Rudst.
79 - 2	34.8	38	98.92	0.10	0.06	0.04	0.82	0.02	0.01	0.00	0.00	0.56	17	Bindst. Floatst. Rudst. (Grainst. Mudst.)
79 - 3	38	41.8	98.29	0.37	0.22	0.09	0.90	0.02	0.02	0.00	0.02		16	Rudst. Floatst. Mudst. (Framest.)
79 - 4	41.8	45.4	98.50	0.26	0.15	0.07	0.89	0.02	0.02	0.00	0.01		16	Framest. Rudst. (Floatst.)
79 - 5	45.4	48.3	98.64	0.22	0.14	0.08	0.81	0.03	0.01	0.00	0.01		16	Mudst. Floatst. (Framest.)
79 - 6	48.3	51.1	98.63	0.18	0.11	0.05	0.91	0.02	0.02	0.00	0.01		16 (15)	Rudst. Framest. (Floatst. Framest.)
79 - 7	51.1	54.1	98.64	0.12	0.08	0.05	1.01	0.03	0.01	0.00	0.01	0.61	15	Bafflest. Framest. (Mudst.)
79 - 8	54.1	56.6	95.78	0.73	0.42	0.27	2.43	0.06	0.02	0.00	0.10		15	Bindst. (Dolost.)
79 - 9	56.6	58.6	98.09	0.51	0.29	0.10	0.72	0.05	0.01	0.00	0.13		15	Bindst. Framest. (Floatst.)
79 - 10	58.6	60.7	98.97	0.10	0.06	0.04	0.76	0.04	0.01	0.00	0.01	0.97	15	Framest.
79 - 11	60.7	67.2	98.72	0.26	0.16	0.09	0.59	0.07	0.01	0.00	0.05		13/14 (15)	Mudst. Floatst. (Bafflest. Bindst. Framest.)
79 - 12	67.2	72.45	98.42	0.34	0.20	0.10	0.77	0.04	0.01	0.00	0.06		13	Mudst. (Bindst. Floatst.)
79 - 13	72.45	76.1	98.76	0.20	0.12	0.06	0.74	0.03	0.01	0.00	0.03		13	Mudst. (Rudst. Bindst.)
79 - 14	76.1	78	93.50	0.32	0.19	0.28	5.46	0.09	0.04	0.00	0.04		12 (13)	Rudst. Floatst. (Mudst. Grainst.)
79 - 15	78	83	98.30	0.35	0.20	0.09	0.89	0.03	0.02	0.00	0.03		12	Rudst. Floatst.
79 - 16	83	86.35	98.07	0.40	0.24	0.09	0.88	0.03	0.02	0.00	0.17		11 (12)	Grainst. (Floatst. Rudst.)
79 - 17	86.35	89.4	98.71	0.17	0.11	0.06	0.87	0.03	0.01	0.00	0.00	0.75	11	Grainst.
79 - 18	89.4	92.8	99.00	0.10	0.07	0.03	0.75	0.02	0.00	0.00	0.01	0.54	10 / 11	Mudst. Grainst. (Floatst.)
79 - 19	92.8	95	98.68	0.14	0.09	0.07	0.93	0.04	0.01	0.00	0.03	0.81	10	Floatst. (Mudst.)
79 - 20	95	97.6	98.79	0.15	0.10	0.06	0.78	0.03	0.01	0.00	0.01	0.79	10	Mudst. Framest. (Floatst.)
79 - 21	97.6	100.6	98.46	0.17	0.11	0.08	1.05	0.03	0.02	0.00	0.01		10	Mudst. Floatst.
79 - 22	100.6	105.2	97.52	0.75	0.46	0.16	0.78	0.03	0.02	0.00	0.09		9 / 10	Mudst. Floatst. (Framest.)
79 - 23	105.2	108	98.88	0.14	0.09	0.04	0.73	0.02	0.02	0.00	0.03	0.70	9	Mudst. Rudst. Bafflest.
79 - 24	108	113.35	98.85	0.16	0.11	0.05	0.71	0.03	0.01	0.00	0.02	0.63	9	Mudst. Rudst. Framest. (Bafflest.)
79 - 25	117	121.4	98.58	0.25	0.15	0.07	0.80	0.03	0.01	0.00	0.01		8	Floatst. (Mudst. Wackest.)
79 - 26	121.4	125.8	94.92	0.35	0.21	0.25	4.06	0.07	0.02	0.00	0.03		8	Floatst. (Mudst. Rudst.)
79 - 27	125.8	130	99.06	0.08	0.06	0.03	0.69	0.03	0.01	0.00	0.01	0.63	(7) 8	Mudst. Floatst. (Grainst.)
79 - 28	130.3	132.1	98.96	0.19	0.13	0.06	0.59	0.04	0.00	0.00	0.02		7	Mudst.
79 - 29	132.1	138.1	96.60	1.23	0.79	0.24	0.75	0.03	0.01	0.00	0.05		7	Packst. Mudst. Rudst. (Grainst.)
79 - 30	138.1	142.75	97.98	0.55	0.36	0.13	0.76	0.04	0.02	0.00	0.01		7	Mudst.
79 - 31	142.75	144.7	98.91	0.11	0.08	0.04	0.73	0.03	0.01	0.00	0.01	0.94	7	Rudst.
79 - 32	144.7	147.3	98.78	0.21	0.13	0.13	0.59	0.10	0.01	0.00	0.02		7	Rudst. Mudst. (Wackest.)
79 - 33	147.3	152.1	98.62	0.13	0.09	0.07	0.99	0.04	0.01	0.00	0.01		6 (7)	Rudst. Bindst. (Mudst. Framest. Wackest.)
79 - 34	152.1	153	98.77	0.28	0.16	0.10	0.58	0.07	0.00	0.01	0.01		6	Rudst.
79 - 35	155	164	98.45	0.17	0.11	0.10	1.02	0.07	0.02	0.01	0.02		(4) 5	Grainst. Rudst. Floatst. Mudst. (Packst.)
79 - 36	164	167.6	81.52	1.17	0.66	0.70	15.28	0.26	0.04	0.02	0.08		4	Rudst. (Mudst. Wackest.)
79 - 37	167.6	171.8	94.54	0.26	0.16	0.33	4.45	0.10	0.02	0.01	0.03		4	Mudst. Rudst. (Floatst. Wackest.)
79 - 38	171.8	173.2	99.03	0.07	0.05	0.03	0.73	0.04	0.01	0.01	0.00	0.64	4	Mudst.
79 - 39	173.2	174.7	95.87	0.15	0.09	0.14	3.61	0.07	0.01	0.01	0.01		4	Mudst.
79 - 40	174.7	179.3	98.06	0.33	0.21	0.09	1.17	0.04	0.02	0.01	0.01		3 (4)	Mudst. Floatst.
79 - 41	179.3	183.2	98.67	0.14	0.09	0.05	0.96	0.03	0.01	0.00	0.01	0.55	3	Mudst. Floatst.
79 - 42	183.2	186	94.30	0.09	0.07	0.19	5.22	0.08	0.02	0.00	0.01		3	Mudst. Floatst. (Wackest.)
79 - 43	186	190.3	98.26	0.13	0.08	0.08	1.33	0.05	0.01	0.01	0.02		2	Mudst. Rudst.
79 - 44	190.3	194.4	97.93	0.48	0.29	0.13	0.89	0.07	0.03	0.01	0.07		2	Mudst. Rudst. Floatst.
79 - 45	194.4	197.1	98.83	0.07	0.05	0.05	0.91	0.04	0.02	0.00	0.00		2	Mudst. Rudst. Floatst.
79 - 46	197.1	200	98.76	0.12	0.08	0.06	0.87	0.04	0.03	0.00	0.00		1 (2)	Bafflest. (Framest. Floatst.)

Table 2 Lithofacies types (FTs) vs depth, documented in the Hahnstätten Reef section. The majority of lithofacies types represent shallow-subtidal, intertidal to supratidal environments, and back reef settings

	Lithofacies	Occurrence (m)	Major components and sedimentological characteristics	Subordinate components and sedimentological characteristics	Matrix	Cements	Palaeoenvironment
FT 1	lime mudstone	32.05-33.05 33.40-34.10 34.95-35.15 35.40-35.45 40.85-41.80 52.90-53.15 61.70-62.40 65.00-68.35 68.70-71.55 71.80-72.25 72.35-73.25 73.50-73.60 73.90-76.40 83.55-83.65 91.20-92.80 93.20-93.35 95.10-95.25 95.80-97.05 97.45-99.25 102.65-105.55 106.05-106.25 106.40-107.45 108.15-109.81 117.00-118.20 124.60-126.80 128.85-132.70 133.25-134.05 138.10-142.70 145.60-145.75 146.45-148.00 152.15-152.35 154.15-154.55 155.90-157.95 165.60-165.85 167.60-169.10 171.70-176.45 185.60-185.70 185.85-185.95 186,00-186,30 186.80-187.50 188.10-190.30 193.20-195.95 196.45-196.75	generell scarcity of biota, shellhash (brachiopods, *Stringocephalus burtini*, ostracods); thamnopora; stylolites	spirally-ribbed pleurotomariid gastropod; pyrite grains; burrows	mud	rare to absent, except rare meniscus cement	low-energy, intertidal to shallow subtidal, lagoonal setting
FT 2a	irregularly laminated fenestral limestone	39.15-39.50 51.70-52.1	algae, laminar stromatoporoids; irregularly, fine-scale laminations, mud intraclasts	benthic foraminifera, ostracods, indistinguishable fragments, irregular fenestral fabric, small fecal pellets	alternation of mud, peloidal layers, and micrite/mud	rare vadose	restricted, shallow-subtidal, intertidal to supratidal environments
FT 2b	regularly laminated fenestral limestone	44.75-46.15	algae, laminar stromatoporoids; regularly, fine-scale laminations, algae fine-grained dolomite	benthic foraminifera, ostracods, indistinguishable fragments	alternation of mud, peloidal layers, and algae	rare vadose	restricted, shallow-subtidal, intertidal to supratidal environments

Table 2 (Continued)

	Lithofacies	Occurrence (m)	Major components and sedimentological characteristics	Subordinate components and sedimentological characteristics	Matrix	Cements	Palaeoenvironment
FT 2c	bindstone	31.75-31.85 34.45-34.95 35.95-37.25 54.10-55.05 55.30-57.95 61.50-61.70 62.40-62.55 68.35-68.70 73.70-73.80 148.25-149.50 150.05-150.10	laminar algae (organic framework); fenestral fabric	brachiopods, rare gastropods	mud, often laminated	marine phreatic and sparry calcite	low-energy, shallow-subtidal, intertidal to supratidal environments
FT 3	wackestone	118.20-119.05 167.30-167.60 171.10-171.30	thamnoporids, alveolitids, ostracods; in parts strongly burrowed, geopetals occur	brachiopods, gastropods, foraminifera; rare conodonts	mixture of lime mudstone and laminated lime mudstone	rare to absent; pore fillings contain radiaxial fibrous cement	shallow lagoonal environments with open water circulation
FT 4	floatstone	40.00-40.85 41.80-42.30 46.15-46.25 47.70-49.00 57.95-58.20 61.10-61.50 62.55-64.80 76.40-76.95 78.20-78.70 79.60-80.20 83.45-83.55 90.90-91.20 92.80-93.20 93.35-95.10 97.05-97.45 99.25-102.10 119.05-123.90 162.45-162.85 169.10-169.45 185.70-185.85 185.95-186.00 191.25-193.20 196.90-197.95	corals (alveolites, thamnopora) stromatoporoids (*Stachyodes*)	brachiopods; pressure solution seams	organic-rich mud to mottled brownish wackestone	rare	low-energy, backreef environment
FT 4a	floatstone	44.55-44.75 71.55-71.80 72.25-72.35	alveolites	stromatoporoids	organic-rich mud to mottled brownish wackestone	rare	low-energy, backreef environment
FT 4b	floatstone	35.45-35.95 84.30-84.45 155.05-155.90	spirally-ribbed pleurotomariid gastropods	corals, stromatoporoids, microbial coating	organic-rich mud to mottled brownish wackestone	rare	low-energy, backreef environment

Table 2 (Continued)

	Lithofacies	Occurrence (m)	Major components and sedimentological characteristics	Subordinate components and sedimentological characteristics	Matrix	Cements	Palaeoenvironment
FT 1 / FT 4	alternation of lime mudstone and floatstone	176.45-185.60	see description for both FTs above	see description for both FTs above	see description for both FTs above	see description for both FTs above	alternation of low-energy back reef and lagoonal environments
FT 5	packstone/ rudstone or rudstone	31.65-31.75 31.85-32.05 34.10-34.45 37.25-39.00 39.50-40.00 42.30-42.85 49.00-50.70 77.20-78.20 78.70-79.60 80.20-83.45 105.55-106.05 106.25-106.40 107.45-107.65 107.95-108.15 109.85-111.20 123.90-124.60 127.10-128.85 132.70-133.25 136.35-137.70 142.70-145.60 145.75-146.45 148.00-148.25 149.50-150.05 150.10-151.80 152.35-153.10 157.95-158.30 161.80-162.45 162.85-165.60 165.85-167.30 169.45-171.10 171.30-171.70 186.30-186.80	tabular and laminar stromatoporoids, corals, densely packed, no gradation	echinoderms (crinoid ossicles), brachiopods, gastropods, sponge spicule; bioclasts are encrusted	lime mudstone to wackestone	minor marine cement	high-energy environment, redeposited in low-energy settings within the reef
FT 6	grainstone	35.15-35.40 76.95-77.20 83.65-84.30 84.45-90.90 126.80-127.10 134.05-136.35 137.70-138.10 158.30-161.80	corals, stromatoporoids, brachiopods; echinoderms bioclastic coatings	gastropods, ostracods, conodonts; peloidal, micritic clasts (angular to rounded)	sparitic matrix, rare micrite (peloidal matrix =peloidal grainstone)	marine cement	shallow-water, high energy setting, shallow subtidal, moderate water circulation
FT 7	baffle stone	52.15-52.90 53.15-54.10 64.80-65.00 107.65-107.95 112.80-113.75 198.15-200.20	domical, ragged stromatoporoids, most are in-situ	corals, algae, brachiopods, foraminifera	biogenic fabrics, lime mudstone in between	mudstone in between mud, minor marine cement except pore fillings	moderately agitated water conditions, rather back-reef setting

Table 2 (Continued)

	Lithofacies	Occurrence (m)	Major components and sedimentological characteristics	Subordinate components and sedimentological characteristics	Matrix	Cements	Palaeoenvironment
FT 8	framestone and framestone/baffle-stone	39.00-39.15 42.85-44.55 50.70-51.70 58.20-61.10 73.25-73.50 73.60-73.70 95.25-95.80 102.10-102.65 111.20-112.80 151.80-152.15 197.95-198.15	stromatoporoids, corals, (organic framework)	brachiopods, rare gastropods, foraminifera, algae	biogenic fabrics, sparitic matrix, rare lime mud	rare mud, large voids contain marine phreatic and sparry calcite	medium-strength water turbulence, reef flat
FT 9	dolostone	55.05-55.30	tabular and laminar stromatoporoids, corals, densely packed or scarcity of biota, shell-hash (brachiopods, ostracods); dolomitization causes obliteration of primary constituents	bulbous stromatoporoids, gastropods gastropods, corals	micrite to sparitic matrix lime mud	marine cement rare	high-energy environment, redeposited in low-energy settings within the reef low-energy, restricted environment

Acknowledgements We thank SCHAEFER KALK GmbH & Co, Hahnstätten, Germany for providing the sample material. This is a contribution to International Geoscience Programmes, IGCP 652 and IGCP 700. We thank Julian Denayer (Liège, Belgium) and an anonymous reviewer for their constructive comments and suggestions, which improved the final version of this manuscript. Furthermore, we thank Jana Anger, Stefanie Hirschmann, and Michael Ricker (Senckenberg Research Institute and Natural History Museum Frankfurt) for preparing thin sections and polished cores.

Funding Open Access funding enabled and organized by Projekt DEAL.

Data availability The material investigated in this study is stored at the Senckenberg Research Institute and Natural History Museum Frankfurt, Germany.

Declarations

Conflict of Interest The authors declare that they have no conflict of interest.

References

Aboussalam, Z.S., & Becker, R.T. (2016). A lower Frasnian reef drowning episode at Walheim (Aachen region, Inde Syncline, NW Rhenish Massif). In R.T. Becker, S. Hartenfels, P. Königshof, & S. Helling (Eds.), Middle Devonian to Lower Carboniferous stratigraphy, facies, and bioevents in the Rhenish Massif, Germany – an IGCP 596 Guidebook. *Münstersche Forschungen zur Geologie und Paläontologie*, *108*, 14–28.

Aharon, P., Socki, R.A., & Chan, L. (1987). Dolomitization of atolls by seawater convection flow: test of a hypothesis at Niue, South Pacific. *Journal of Geology*, *95*, 187–203.

Becker, R.T., Aboussalam, Z.S., Hartenfels, S., Nowak, H., Juch, D., & Drozdzewski, G. (2016a). Drowning and sedimentary cover of Velbert Anticline reef complexes (northwestern Rhenish Massif). In R.T. Becker, S. Hartenfels, P. Königshof, & S. Helling (Eds.), Middle Devonian to Lower Carboniferous stratigraphy, facies, and bioevents in the Rhenish Massif, Germany – an IGCP 596 Guidebook. *Münstersche Forschungen zur Geologie und Paläontologie*, *108*, 76–101.

Becker, R.T., Königshof, P., & Brett, C.E. (2016b). Devonian climate, sea level and evolutionary events: an introduction. In R.T. Becker, P. Königshof, & C.E. Brett (Eds.), Devonian Climate,

Sea Level and Evolutionary Events. *Geological Society, London, Special Publication*, *423*, 1–10.

Braun, R., Oetken, S., Königshof, P., Kornder, L., & Wehrmann, A. (1994). Development and biofacies of reef-influenced carbonates (Lahn Syncline, Rheinisches Schiefergebirge). *Courier Forschungsinstitut Senckenberg, 169*, 351–386.

Brett, C.E., Baird, G.C., Bartholomew, A.J., DeSantis, M.K., & Ver-Straeten C.A. (2011). Sequence stratigraphy and a revised sea-level curve for the Middle Devonian of eastern North America. In C.E. Brett, E. Schindler, & P. Königshof (Eds.), Sea-level cyclicity, climate change, and bioevents in Middle Devonian marine and terrestrial environments. *Palaeogeography, Palaeoclimatology, Palaeoecology, 304*, 21–53.

Buggisch, W., & Flügel, E. (1992). Mittel- bis oberdevonische Karbonate auf Blatt Weilburg (Rheinisches Schiefergebirge) und in Randgebieten: Initialstadien der Riffentwicklung auf Vulkanschwellen. *Geologisches Jahrbuch Hessen, 120*, 77–97.

Bultynck, P. (1970). Révision stratigraphique et paléontologique (Brachiopodes et Conodontes) de la coupe type du Couvinien. *Mémoires de l'Institut Géologique de l' Université de Louvain*, *26*, 1–52.

Bultynck, P. (1987). Pelagic and neritic conodont successions from the Givetian of pre-Sahara Morocco and the Ardennes. *Bulletin de l' Institute Royal des Sciences Naturelles de Belgique, Sciences de la Terre, 57*, 149–181.

Carballo, J.D., Land, L.S., & Miser, D.E. (1987). Holocene dolomitization of supratidal sediments by active tidal pumping, Sugarloaf Key, Florida. *Journal of Sedimentary Petrology, 57*, 153–165.

Choquette, P.W., & Hiatt, E.E. (2008). Shallow-burial dolomite cement: A major component of many ancient sucrosic dolomites. *Sedimentology, 55*(2), 423–460.

Copper, P. (2002a). Silurian and Devonian reefs: 80 million years of global greenhouse between two ice ages. *SEPM Special Publication, 72*, 181–238.

Copper, P. (2002b). Reef development at the Frasnian/Famennian mass extinction boundary. *Palaeogeography, Palaeoclimatology, Palaeoecology, 181*, 27–65.

Copper, P., & Scotese, C.R. (2003). Megareefs in Middle Devonian supergreenhouse climates. In M.A. Chan, & A.W. Archer (Eds.), Extreme depositional environments: Mega end members in geologic time. *Geological Society of America, Special Paper*, *370*, 209–230.

Da Silva, A.C., & Boulvain, F. (2004). From palaeosols to carbonate mounds: facies and environments of the middle Frasnian platform in Belgium. *Geological Quarterly*, *48*, 253–266.

Drzwiecki P.A., & Simo, J.A. (1997). Carbonate Platform Drowning and Oceanic Anoxic Events on a Mid-Cretaceous Carbonate Platform, South-Central Pyrenees, Spain. *Journal of Sedimentary Research*, *67*(4), 689–714.

Eder, W., & Franke, W. (1982). Death of Devonian reefs. *Neues Jahrbuch für Geologie und Paläontologie, Abhandlungen*, *163*(2), 241–243.

Eisenlohr, H. (1983) Ein typisches Beispiel für die Verkarstung der Oberfläche von devonischen Massenkalken im Lahngebiet. *Erwin Rutte-Festschrift*, 61–64; Kelheim/Weltenburg (Weltenburger Akademie).

Elrick, M., Berkyová, S., Klapper, G., Sharp, Z., Joachimski, M., & Frýda, J. (2009). Stratigraphic and oxygen isotope evidence for My-scale glaciation driving eustasy in the Early-Middle Devonian greenhouse world. *Palaeogeography, Palaeoclimatology, Palaeoecology*, *276*, 170–181.

Embry, A.F., & Klovan, E.J. (1971). A Late Devonian reef tract on Northeastern Banks Island, NWT. *Bulletin of Canadian Petroleum Geology*, *19*, 730–781.

Epstein, A.G., Epstein, J.B., & Harris, L.D. (1977). Conodont colour alteration – an index to organic metamorphism. *Geological Survey of America, Professional Paper*, *995*, 1–27.

Faber, P. (1980). Fazies-Gliederung und -Entwicklung im Mitteldevon der Eifel (Rheinisches Schiefergebirge). *Mainzer geowissenschaftliche Mitteilungen*, *8*, 83–149.

Fåhræus, L.E., Slatt, R.M., & Nowlan, G.S. (1974). Origin of carbonate pseudopellets. *Journal of Sedimentary Petrology*, *44*(1), 27–29.

Flick, H., & Nesbor, H.D. (2021) 3.3. Lahn-Dill-Gebiet. In B. Becker, & T. Reischmann (Eds.), *Geologie von Hessen* (pp. 49–77). Stuttgart: E. Schweizerbart`sche Verlagsbuchhandlung (Nägele und Obermiller).

Flügel, E. (2004). *Microfacies of Carbonate Rocks*. Analysis Interpretation and Application (pp. 1–976). Berlin: Springer-Verlag.

Flügel, E., & Kiessling, W. (2002). Patterns of Phanerozoic reef crisis. In W. Kiessling, E. Flügel, & J. Golonka (Eds.), Phanerozoic reef patterns. *SEPM Special Publication*, *72*, 691–733.

Föllmi, K.B., Weissert, H., Bisping, M., & Funk, H. (1994). Phosphogenesis, carbon–isotope stratigraphy, and carbonate–platform evolution along the Lower Cretaceous northern Tethyan margin. *Geological Society of America Bulletin*, *106*, 729–746.

Garland, J., Tucker, M.E., & Scrutton, C.T. (1996). Microfacies analysis and metre-scale cyclicity in the Givetian back-reef sediments of south-east Devon. *Proceedings of the Ussher Society*, *9*, 31–36.

Gischler, E. (1995). Current and wind induced facies patterns in a Devonian atoll, Iberg Reef, Harz Mts., Germany. *Palaios, 10*, 180–189.

Hallam, A., & Wignall, P.B. (1997). *Mass extinctions and their aftermath* (pp. 1-320). Oxford, UK: Oxford University Press.

Hallock, P., & Schlager, W. (1986). Nutrient excess and the demise of coral reefs and carbonate platforms. *Palaios*, *1*, 389–398.

Hartkopf-Fröder, C., & Weber, H.M. (2016). From Emsian coastal to Famennian marine environments: palaeogeographic evolution and biofacies in the Bergisch Gladbach-Paffrath Syncline area (Rhenish Massif, Germany). In R.T. Becker, S. Hartenfels, P. Königshof, & S. Helling (Eds.), *Middle Devonian to Lower Carboniferous stratigraphy, facies, and bioevents in the Rhenish Massif, Germany – an IGCP 596 Guidebook*. *Münstersche Forschungen zur Geologie und Paläontologie*, *108*, 46–75.

Haq, B.U., & Schutter, S.R. (2008). A chronology of Palaeozoic sea-level changes. *Science*, *322*, 64–68.

Hinde, G.J. (1879). On conodonts from the Chazy and Cincinnati Group of the Cambro-Silurian, and from the Hamilton and Geneseee-Shale divisions of the Devonian, in Canada and the United States. *Geological Society London, Quarterly Journal, 35,* 351–369.

Hofmann, M.H., & Keller, M. (2006). Sequence stratigraphy and carbonate platform organization of the Devonian Santa Lucia Formation, Cantabrian Mountains, NW Spain. *Facies*, *52*, 149–167.

Joachimski, M.M., Breisig, S., Buggisch, W., Mawson, R., Gereke, M., Morrow, J.R., Day, J., & Weddige, K. (2009). Devonian climate and reef evolution: insights from oxygen isotopes in apatite. *Earth and Planetary Science Letters*, *284*, 599–609.

John, D.K. (2012). Controls on lithofacies variability in Late Devonian, Cynthia Basin reefs, Nisku Formation, Western Canadian Sedimentary Basin (pp. 128). *Master Thesis, Queen`s University Kingston, Ontario, Canada*.

Johnson, J.G., Klapper, G., & Sandberg, C.A. (1985). Devonian eustatic fluctuations in Euramerica. *Geological Survey of America, Bulletin, 96*, 567–587.

Kershaw, S., & Keeling, M. (1994). Factors controlling the growth of stromatoporoid biostroms in the Ludlow of Gotland, Sweden. *Sedimentary Geology*, *89*, 325–335.

Kershaw, S., & Riding, R. (1978). Parameterisation of stromatoporoid shape. *Lethaia*, *11*, 233–244.

Klapper, G., Philip, G.M., & Jackson, J.H. (1970). Revision of the Polygnathus varcus group (Conodonta, Middle Devonian). *Neues Jahrbuch für Geologie und Paläontologie, Monatshefte 1970* (11), 1650–1667

Koch-Früchtl, U., & Früchtl, M. (1993). Stratigraphie und Faziesanalyse einer mitteldevonischen Karbonatabfolge im Remscheid-Altenaer Sattel (Sauerland). *Geologie und Paläontologie in Westfalen*, *26*, 47–75.

Königshof, P. (2003). Conodont deformation patterns and textural alteration in Paleozoic conodonts: examples from Germany and France. *Senckenbergiana lethaea*, *83*(1/2), 149–156.

Königshof, P., & Flick, H. (in press) Fringing reef growth vs. volcanism: An example from the Rhenish Massif, Germany. In S. Hartenfels, C. Hartkopf-Fröder, & P. Königshof (Eds.) *The Rhenish Massif: More than 150 years of research in a Variscan mountain chain, part II. Palaeobiodiversity and Palaeoenvironments.* [this issue]

Königshof, P., & Kershaw, S. (2006). Growth forms and palaeoenvironmental interpretation of stromatoporoids in a Middle Devonian reef, southern Morocco (west Sahara). *Facies, 52*(2), 299–306.

Königshof, P., Gewehr, B., Kornder, L., Wehrmann, A., Braun, R., & Zankl, H. (1991). Stromatoporen-Morphotypen aus einem zentralen Riffbereich (Mitteldevon) der südwestlichen Lahnmulde. *Geologica et Palaeontologica*, *25*, 19–35.

Königshof, P., Nesbor H.D., & Flick, H. (2010). Volcanism and reef development in the Devonian: a case study from the Rheinisches Schiefergebirge (Lahn Syncline, Germany). *Gondwana Research*, *17*, 264–280. https://doi.org/10.1016/j.gr.2009.09.006.

Königshof, P., Helling, S., Hartenfels, S., DeVleeschouwer, D., Schreiber, G., Becker, R.T., & Brett, CB. (2016). Eifel Synclines – an overview and Emsian to Frasnian section descriptions. In R.T. Becker, S. Hartenfels, P. Königshof, & S. Helling (Eds.), *Middle Devonian to Lower Carboniferous stratigraphy, facies, and bioevents in the Rhenish Massif, Germany – an IGCP 596 guidebook*. *Münsterische Forschungen zur Geologie und Paläontologie*, *108*, 36–45.

Königshof, P., Jansen, U., Linnemann, U., & Mende, K., (2023). The Rhenish Massif. In U. Linnemann (Ed.), *Geology of the Variscan Orogen in Central and Eastern Europe – From the margin of Gondwana to the center of Pangea.* Springer. [in press]

Krebs, W. (1971). Die devonischen Riffe in Mitteleuropa. *Mitteilungen der Technischen Universität Carolo-Wilhelmina zu Braunschweig*, *6*(2/3), 22–33.

Krebs, W. (1974). Devonian carbonate complexes of Central Europe. In L. F. Laporte (Ed.), Reefs in time and space. *SEPM, Special Publication*, *18*, 155–208.

Liao, J.C., & Valenzuela-Rios, J.I. (2008). Givetian and early Frasnian conodonts from the Compte section (Middle-Upper Devonian, Spanish Central Pyrenees). *Geological Quarterly, 52*(1), 1–18.

Löw, M., Söte, T., Becker, R. T., May, A., & Stichling, S. (2022). Microfauna and microfacies from the initial reef stadium of Binolen in the Hönne Valley (Sauerland, Middle Devonian). In S. Hartenfels, C. Hartkopf-Fröder, & P. Königshof (Eds.), *The Rhenish Massif: More than 150 years of research in a Variscan mountain chain. Palaeobiodiversity and Palaeoenvironments, 102*(3), 573–612. https://doi.org/10.1007/s12549-022-00540-4.

Machel, H.G., & Hunter, I.G. (1994). Facies models for Middle to Late Devonian shallow-marine carbonates, with comparisons to modern reefs: a guide for facies analysis. *Facies*, *30*, 155–176.

MacNeil, A.J., & Jones, B. (2016). Stromatoporoid growth forms and Devonian reef fabrics in the Upper Devonian Alexandra Reef System, Canada – Insight on challenges of applying Devonian reef facies models. *Sedimentology*, *63*, 1425–1457.

Malmsheimer, K.W., Mensink, H., & Stritzke, R. (1991). Gesteinsvielfalt im Riffgebiet um Brilon. *Geologie und Paläontologie in Westfalen*, *18*, 67– 83.

Mestermann, B. (1995). Fenstergefüge im südlichen Briloner Massenkalk. *Geologie und Paläontologie in Westfalen*, *41*, 55–67.

Mottequin, B., & Poty, E. (2016). Kellwasser horizons, sea-level changes and brachiopod-coral crises during the late Frasnian in the Namur-Dinant Basin (southern Belgium): a synopsis. In R.T. Becker, P. Königshof, & C.E. Brett (Eds.), *Devonian Climate, Sea Level and Evolutionary Events*. *Geological Society, London, Special Publications*, *423*, 235–250.

Mottequin, B., Denayer, J., Poty, E., & Devleeschouwer, X. (2015). Middle to Upper Frasnian succession, Kellwasser events and the Frasnian–Famennian Boundary in the Namur–Dinant Basin. In J. Denayer, B. Mottequin, & C. Prestianni (Eds.), *IGCP 596 - SDS Symposium, Climate change and Biodiversity patterns in the Mid-Palaeozoic, Field Guidebooks. Strata*, *Travaux de Géologie sédimentaire et Paléontologie, Serié 1: communications*, *17*, 24–45.

Narkiewicz, K., & Königshof, P. (2018). New Middle Devonian conodont data from the Dong Van area, NE Vietnam (South China Terrane). *Paläontologische Zeitschrift, 92*(4), 633–650. https://doi.org/10.1007/s12542-018-0408-6.

Nesbor, H.D. (1984). *Geologische Kartierung in der Katzenelnbogen-Hahnstätter Mulde/südwestliche Lahnmulde (südliches Rheinisches Schiefergebirge)* (pp. 84). Heidelberg: Diplom Kartierung Universität Heidelberg.

Nesbor, H.D. (2008). Bimodaler Vulkanismus im Devon des Rheinischen Schiefergebirges. In Deutsche Stratigraphische Kommission (Hrsg.). Stratigraphie von Deutschland VIII. Devon. *Schriftenreihe der Deutschen Gesellschaft für Geowissenschaften Heft, 52*, 247–251.

Nesbor, H.D., Buggisch, W., Flick, H., Horn, M., & Lippert, H.J. (1993). Fazielle und paläogeographische Entwicklung vulkanisch geprägter mariner Becken am Beispiel des Lahn-Dill-Gebietes. *Geologische Abhandlungen Hessen*, *98*, 3–87.

Oetken, S. (1997). Faziesausbildung und Conodonten-Biofazies mittel-/ oberdevonischer Riffgesteine in der mittleren Lahnmulde (Rheinisches Schiefergebirge). *Wissenschaft in Dissertationen*, *207*, 1–161.

Pohler, S.M.L., Brühl, D., & Mestermann, B. (1999). Struves mud mound am Weinberg – carbonate buildup-Fazies im *otomari*-Interval, Hillesheimer Mulde, Eifel. *Senckenbergiana lethaea*, *79*, 13–29.

Pratt, B.R. (2011). Peritidal Carbonates. In N.P. James, & R.W. Dalrymple (Eds.), *Facies Model 4* (pp. 1-586). *St. John`s Newfoundland, Geological Association of Canada*.

Requadt, H. (2008). Südwestliche Lahnmulde (Rheinland-Pfalz). In Deutsche Stratigraphische Kommission (Ed.), *Stratigraphie von Deutschland VIII. Devon. Schriftenreihe der Deutschen Gesellschaft für Geowissenschaften, SDGG, Stratigraphie von Deutschland 52*, 204–220.

Riding, R.E. (1981). Composition, structure and environmental setting of Silurian bioherms and biostroms in Northern Europe. *SEPM Special Publication*, *30*, 41–83.

Schudack, M.E. (1993). Karbonatzyklen in Riff- und Lagunenbereichen des devonischen Massenkalkkomplexes von Asbeck (Hönnetal, Rheinisches Schiefergebirge). *Geologie und Paläontologie in Westfalen*, *26*, 77–106.

Stearn, C.W. (2016). The shapes of Paleozoic and modern reef-builders: a critical review. *Paleobiology, 8*(3), 228–241.

Stearn, C.W., Webby, B.D., Nestor, H., & Stock, C.W. (1999). Revised classification and terminology of Palaeozoic stromatoporoids. *Acta Palaeontologica Polonica, 44*, 1–70.

Stichling, S., Becker, R.T, Hartenfels, S., Aboussalam, Z.S., & May, A. (2022). Drowning, extinction, and subsequent facies development of the Devonian Hönne Valley Reef (northern Rhenish Massif, Germany). In S. Hartenfels, C. Hartkopf-Fröder, & P. Königshof (Eds.), *The Rhenish Massif: More than 150 years of research in a Variscan mountain chain. Palaeobiodiversity and*

Palaeoenvironments, *102*(3), 629–696. https://doi.org/10.1007/s12549-022-00539-x.

Ta, H.P., Königshof, P., Ellwood, B.B., Luu, T.P.L., Nguyen, C.T., Huong Doan, D., & Munkhjargal, A. (2022). Facies, magnetic susceptibility and timing of the Late Devonian Frasnian/Famennian boundary interval (Xom Nha Formation, Central Vietnam). *Palaeobiodiversity and Palaeoenvironments*, *102*(3), 129–146. https://doi.org/10.1007/s12549-021-00506-y.

Van Geldern, R., Joachimski, M.M., Day, J., Jansen, U., Alvarez, F., Yolkin, E.A., & Ma, X.P. (2006). Carbon, oxygen and strontium isotope records of Devonian brachiopod shell calcite. *Palaeogeography, Palaeoclimatology, Palaeoecology*, *240*, 47–67.

Weller, H. (1991). Facies and development of the Devonian (Givetian/Frasnian) Elbingerode Reef Complex in the Harz Area (Germany). *Facies*, *25*, 1–50.

Wehrmann, A., Blieck, A., Brocke, R., Hertweck, G., Jansen, U., Königshof, P., Plodowski, G., Schindler, E., Schultka, S., & Wilde, V. (2005). Palaeoenvironment and palaeoecology of intertidal deposits in a Lower Devonian siliciclastic sequence of the Mosel Region, Germany. *Palaios, 20*, 101–120.

Whalen, M.T., Day, J., Eberli, G.P., & Homewood, P.W. (2002). Microbial carbonates as indicators for environmental change and biotic crisis in carbonate systems: example from the Late Devonian, Alberta Basin, Canada. *Palaeogeography, Palaeoclimatology, Palaeoecology*, *181*, 127–151.

Wilson, J. L. (1975). *Carbonate facies in geologic history* (pp. 1-471). New York: Springer.

Wittekindt, H. (1966). Zur Conodonten-Chrononologie des Mitteldevons. *Fortschritte in der Geologie von Rheinland und Westfalen, 9*(1), 621–646.

Wood, R. (1999). *Reef Evolution* (pp. 1- 414). New York: Oxford University Press Inc.

Wright, V.P. (1992). A revised classification of reef limestones. *Sedimentary Geology, 76*, 177–186.

Ziegler, W., Klapper, G., & Johnson, J.G. (1976). Redefinition and subdivision of the *varcus*-Zone (Conodonts, Middle-? Upper Devonian in Europe and North America. *Geologica et Palaeontologica*, *10*, 109–140.